The Plant Cell, Vol. 25: 4421–4438, November 2013, www.plantcell.org

The Dual Functions of WLIM1a in Cell Elongation and Secondary Wall Formation in Developing Cotton Fibers[C][W]

Li-Bo Han,[a,b,1] Yuan-Bao Li,[a,b,1] Hai-Yun Wang,[a,b] Xiao-Min Wu,[a,b] Chun-Li Li,[a] Ming Luo,[c] Shen-Jie Wu,[d] Zhao-Sheng Kong,[a,b] Yan Pei,[c] Gai-Li Jiao,[d] and Gui-Xian Xia[a,b,2]

[a] Institute of Microbiology, Chinese Academy of Sciences, Beijing 100101, China
[b] State Key Laboratory of Plant Genomics, Beijing 100101, China
[c] Biotechnology Research Center, Southwest University, Chongqing 404100, China
[d] Institute of Cotton, Shanxi Academy of Agricultural Sciences, Yuncheng 044000, China

ORCID IDs: 0000-0001-7068-8160 (L.H.); 0000-0001-7238-2261 (Y.L.); 0000-0003-4426-9784 (G.X.).

LIN-11, Isl1 and MEC-3 (LIM)-domain proteins play pivotal roles in a variety of cellular processes in animals, but plant LIM functions remain largely unexplored. Here, we demonstrate dual roles of the *WLIM1a* gene in fiber development in upland cotton (*Gossypium hirsutum*). *WLIM1a* is preferentially expressed during the elongation and secondary wall synthesis stages in developing fibers. Overexpression of *WLIM1a* in cotton led to significant changes in fiber length and secondary wall structure. Compared with the wild type, fibers of *WLIM1a*-overexpressing plants grew longer and formed a thinner and more compact secondary cell wall, which contributed to improved fiber strength and fineness. Functional studies demonstrated that (1) WLIM1a acts as an actin bundler to facilitate elongation of fiber cells and (2) WLIM1a also functions as a transcription factor to activate expression of Phe ammonia lyase–box genes involved in phenylpropanoid biosynthesis to build up the secondary cell wall. WLIM1a localizes in the cytosol and nucleus and moves into the nucleus in response to hydrogen peroxide. Taken together, these results demonstrate that WLIM1a has dual roles in cotton fiber development, elongation, and secondary wall formation. Moreover, our study shows that lignin/lignin-like phenolics may substantially affect cotton fiber quality; this finding may guide cotton breeding for improved fiber traits.

INTRODUCTION

The cotton (*Gossypium hirsutum*) fiber develops from a single epidermal cell of the seed coat. Fiber development can be divided into four overlapping stages: initiation, elongation, secondary wall deposition, and maturation (Graves and Stewart, 1988). Mature cotton fiber cells are extremely long, up to 3 to 5 cm, and are occupied in major part by a secondary wall that consists of mainly of cellulose (>90%) and some minor noncellulosic carbohydrates, such as xyloglucans, pectic polysaccharides, xylans, glucomannans, and glucans (Meinert and Delmer, 1977; Huwyler et al., 1979). Owing to its exceptional cell length and simple secondary cell wall composition, the cotton fiber provides an excellent model for studies of plant cell elongation and cell wall biogenesis (Kim and Triplett, 2001). During recent years, significant progress has been made in large-scale identification of genes and proteins involved in fiber development, particularly those related to fiber elongation (Arpat et al., 2004; Shi et al., 2006; Gou et al., 2007; Q.Q. Wang et al., 2010; Zhao et al., 2010; X.M. Li et al., 2013), and a few fiber elongation-related genes have been structurally or functionally characterized (Ruan et al., 2003; Li et al., 2005; Zhang et al., 2011; Xu et al., 2013). However, to date, little is known about the genes and molecular mechanisms governing secondary wall formation.

Lignin is a complex aromatic heteropolymer consisting of three major phenylpropanoid monomers (Boerjan et al., 2003). In vascular plants, lignin is an important component of secondary walls where it acts as natural glue, cross-linking cellulose microfibrils to provide mechanical support to plant tissues (Liu, 2012). Recent molecular and genetic studies revealed that the biosynthesis of secondary wall lignin phenolics is activated via a transcriptional regulatory network (Zhong and Ye, 2007; Zhao and Dixon, 2011). Unlike fiber cells of other plants, the cotton fiber cell has been considered to have no lignin deposition in its secondary wall (Kim and Triplett, 2001). However, several recent studies seem to require that we update this notion. For example, Fan et al. (2009) reported that lignin-like phenolics were present in cotton fibers, and the cinnamyl alcohol dehydrogenase (*CAD*) genes encoding the key enzymes involved in monolignol biosynthesis were highly expressed during the secondary wall synthesis stage. In addition, transcriptome analyses revealed that genes encoding components of the phenylpropanoid pathway are expressed in developing fiber cells (Gou et al., 2007; Al-Ghazi et al., 2009), and the microRNA GhmiR397, targeting the laccase gene involved in lignin polymerization, was found in fiber initials (Wang et al., 2012). Data from all of these studies lead to the hypothesis that lignin or lignin-like phenolics are synthesized in cotton fibers. Identification of fiber-specific gene(s) that may regulate biosynthesis of lignin/lignin-like phenolics, and investigation of their functions in secondary cell wall

[1] These authors contributed equally to this work.
[2] Address correspondence to xiagx@im.ac.cn.
The author responsible for distribution of materials integral to the findings presented in this article in accordance with the policy described in the Instructions for Authors (www.plantcell.org) is: Gui-Xian Xia (xiagx@im.ac.cn).
[C] Some figures in this article are displayed in color online but in black and white in the print edition.
[W] Online version contains Web-only data.
www.plantcell.org/cgi/doi/10.1105/tpc.113.116970

formation will certainly help to verify the presence of such phenolics in fiber cells and, more importantly, to understand the contribution of phenolics to the development of secondary wall properties and fiber quality.

LIN-11, Isl1 and MEC-3 (LIM)-domain proteins are widely distributed in eukaryotes ranging from yeast (*Saccharomyces cerevisiae*) to humans (Dawid et al., 1995). In animal cells, these proteins are distributed in the cytosol, the nucleus, or in both subcellular compartments. The nuclear LIM-domain proteins act primarily in tissue-specific gene regulation and cell fate determination, whereas the cytoplasmic LIM-domain proteins function mainly in cytoskeletal organization (Zheng and Zhao, 2007). Some LIM-domain proteins have both cytoplasmic and nuclear functions and shuttle between the cytoplasm and nucleus (Boateng et al., 2009; Moes et al., 2013). Based on these features of LIM-domain proteins, it has been proposed that LIM-domain proteins may mediate communication between the cytoplasm and the nucleus (Weiskirchen and Günther, 2003).

The first known plant LIM-domain protein, PLIM1, was identified from sunflower (*Helianthus annuus*) pollen (Baltz et al., 1992a, 1992b). Subsequently, LIM-domain proteins have been identified from a number of plant species, such as tobacco (*Nicotiana tabacum*), lily (*Lilium longiflorum*), *Arabidopsis thaliana*, and cotton (Luo et al., 2003; Thomas et al., 2006; Arnaud et al., 2007; Wang et al., 2008; Y. Li et al., 2013). Plant LIM-domain proteins belong to the Cys-rich protein subfamily of animal LIM-domain proteins. They are small proteins of around 200 amino acids and have two LIM domains that are separated by a long (40 to 50 amino acid) linker (Weiskirchen and Günther, 2003). *Arabidopsis* and tobacco LIM-domain proteins can be characterized into two groups: The PLIMs, which are specifically expressed in pollen grains, and the WLIMs, which are expressed in all tissues (Eliasson et al., 2000). While most of the characterized plant LIM-domain proteins showed actin bundling activity, two tobacco LIMs (WLIM1 and WLIM2) exhibited functions in both actin organization and transcriptional activation. Tobacco WLIM1 (Nt-LIM1) was found to bind specifically to the Phe ammonia lyase (PAL)–box element and activate the expression of a β-glucuronidase gene placed under the control of the promoter of the horseradish peroxidase C2 (prxC2) gene (Kaothien et al., 2002) in the phenylpropanoid biosynthesis pathway (Kawaoka et al., 2000; Kawaoka and Ebinuma, 2001), and tobacco WLIM2 was shown to bind to the octameric *cis*-elements (Oct) and activate the expression of the basal histone gene involved in cell proliferation and cell cycle progression (Moes et al., 2013). In addition, several plant LIM-domain proteins, including tobacco WLIM1 and WLIM2, sunflower WLIM1, and *Arabidopsis* LIMs, have cytoplasmic-nuclear localization, and tobacco WLIM2 was shown to shuttle to the nucleus upon cytoskeleton remodeling (Brière et al., 2003; Thomas et al., 2006; Papuga et al., 2010; Moes et al., 2013). Although these results provide important evidence for the subcellular distribution, cytoskeletal function, and transcription factor functions of some plant LIMs, our understanding of the physiological relevance of the plant LIM-domain proteins remains limited.

In this study, we characterized the functions of the cotton WLIM1a protein. We show that WLIM1a has cytoplasmic and nuclear localization and exerts dual functions. On one hand, WLIM1a binds the actin cytoskeleton to bundle actin filaments, which is favorable for fiber cell elongation. On the other hand, WLIM1a binds to the PAL-box DNA element to enhance the transcription of PAL-box genes and stimulates the biosynthesis of lignin/lignin-like phenolics, which is crucial for secondary wall formation. Furthermore, we observed that WLIM1a could shuttle into the nucleus, and hydrogen peroxide (H_2O_2) served as a trigger. Interestingly, we found that a simultaneous improvement in fiber fineness and strength occurred along with the WLIM1a-mediated increase in lignin/lignin-like phenolics content. These results may provide a promising strategy for concurrent improvement of fiber properties by genetic manipulation.

RESULTS

Cloning of *WLIM1a* and Expression Pattern Analysis

We identified four cotton homologs of *Arabidopsis LIM* genes by performing database searches. The phylogenetic relationships of these cotton LIMs, together with Gh-WLIM5 identified by Y. Li et al. (2013), were compared with LIMs from *Arabidopsis*. The result shows that these cotton LIM-domain proteins all belong to the WLIM subgroup. Three of these proteins are homologs of *Arabidopsis* WLIM1 and two are homologs of *Arabidopsis* WLIM2a and WLIM2b. Hence, we designated the four LIMs we identified as WLIM1a, WLIM1b, WLIM1c, and WLIM2a, respectively (Figure 1A; see Supplemental Data Set 1 online). To identify *LIM* genes that are preferentially expressed in cotton fibers, we used quantitative RT-PCR (qRT-PCR) to analyze the expression patterns of the four *WLIMs*. The results showed that these *WLIM* genes were differentially expressed in cotton organs and that *WLIM1a* was expressed preferentially in cotton fiber cells and was also abundant in the stem (Figures 1B to 1E). To further understand the expression specificity of *WLIM1a*, we investigated the expression profile of *WLIM1a* in developing fibers. As shown in Figure 1F, *WLIM1a* expression occurred during the elongation and secondary wall synthesis stages (6 to 24 d postanthesis [DPA]), indicating that its expression is associated with fiber elongation and secondary wall biogenesis.

The full-length cDNA of *WLIM1a* (JX648310) was cloned through 5′ rapid amplification of cDNA ends (RACE). The predicted WLIM1a protein consists of 190 amino acids and contains two typical LIM domains (domain1 and domain2) that are separated by a 44–amino acid linker sequence.

WLIM1a Function Is Associated with Fiber Length Development

Both gain- and loss-of-function approaches were applied to characterize the cellular function of WLIM1a. For the gain-of-function strategy, we generated cotton plants overexpressing *WLIM1a* by cloning the *WLIM1a* cDNA in sense orientation under the control of the cauliflower mosaic virus 35S promoter and introducing the construct into cotton via *Agrobacterium tumefaciens*–mediated transformation. Similarly, for the loss-of-function strategy,

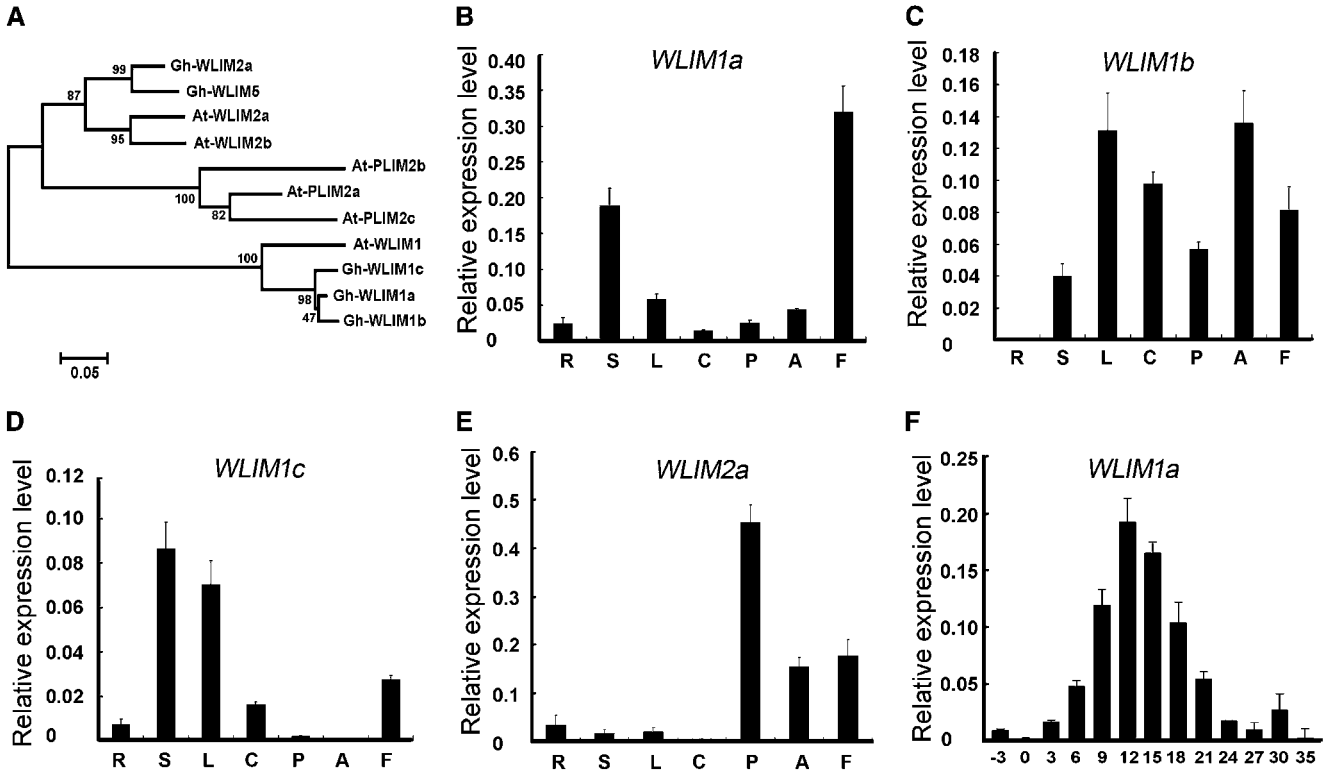

Figure 1. Phylogenetic Relationships of Cotton and *Arabidopsis* LIMs and Expression Patterns of Cotton *WLIMs.*

(A) Phylogenetic tree showing the relationships between cotton and *Arabidopsis* LIM-domain proteins. The numbers on the nodes indicate the confidence values using 1000 replications. The alignment is available as Supplemental Data Set 1 online. At, *Arabidopsis thaliana*; Gh, *Gossypium hirsutum*.
(B) to **(E)** qRT-PCR analysis of *WLIM* gene expression in root (R), stem (S), leaf (L), cotyledon (C), petal (P), anther (A), and fiber (F; 12 DPA) in cotton plants. The expression levels are indicated relative to cotton *UBI*. Error bars represent ±SE of three biological replicates.
(F) qRT-PCR analysis of *WLIM1a* expression in cotton fibers at different developmental stages. −3, 0, 3, Ovules from −3 to 3 DPA; 6 to 35, fibers from 6 to 35 DPA. Error bars represent ±SE of three biological replicates.

the *WLIM1a* cDNA was cloned in antisense orientation. For subsequent analyses, we selected three independent lines of transgenic plants for either *WLIM1a* overexpression (lines 406, 286, and 41) or *WLIM1a* underexpression (lines A1, A2, and A38). We confirmed the up- or downregulation of *WLIM1a* expression in these transgenic lines by qRT-PCR (Figures 2A and 2B). Phenotypic examination showed no significant differences in overall growth and development between the wild type and the two types of transgenic plants except that *WLIM1a*-overexpressing plants exhibited some increases in the length of the peduncle and peduncle trichomes and in the thickness of the stem (see Supplemental Figure 1 online). As *WLIM1a* is expressed preferentially in fiber cells, we then inspected the effects of *WLIM1a* on fiber growth and found obvious change in fiber length in the overexpressing lines (Figure 2C). Quantitative analysis indicated that the fibers of lines 406, 286, and 41 were 10.6, 9.9, and 9.6% longer than the wild type, respectively (Figure 2E). The *WLIM1a*-underexpressing lines did not exhibit an obvious alteration in fiber length (Figures 2D and 2F) or in other fiber properties described below (see Supplemental Figures 2 and 3 online), implying a functional redundancy of *LIM* genes in cotton plants.

Overexpression of *WLIM1a* Alters the Architecture of the Secondary Cell Wall

As the secondary cell wall occupies the major part of the mature cotton fiber, we next inspected the wall structure of wild-type and *WLIM1a*-overexpressing fibers. To our surprise, the cross sections of the transgenic fiber cells showed a dramatic decrease in the thickness and perimeters of the secondary cell wall (Figure 3A). For example, the median thickness of the wild-type fiber was 6.14 μm, whereas the transgenic fibers were 4.63, 4.74, and 4.91 μm for lines 406, 286, and 41, respectively (Figure 3C). To see this change more clearly, we used transmission electron microscopy to view longitudinal sections of mature and 30-DPA fibers and found that the secondary walls of the transgenic fibers were much thinner and appeared more compact than those of the wild-type cells (Figure 3B). As the secondary wall is built up with an ordered array of cellulose microfibrils and their deposition pattern is a major determinant of cell wall properties (Emons and Mulder, 2000), we also measured this parameter by x-ray diffraction and found that the microfibrils angles were reduced in the transgenic fibers compared with the wild-type control (Table 1). Scanning electron

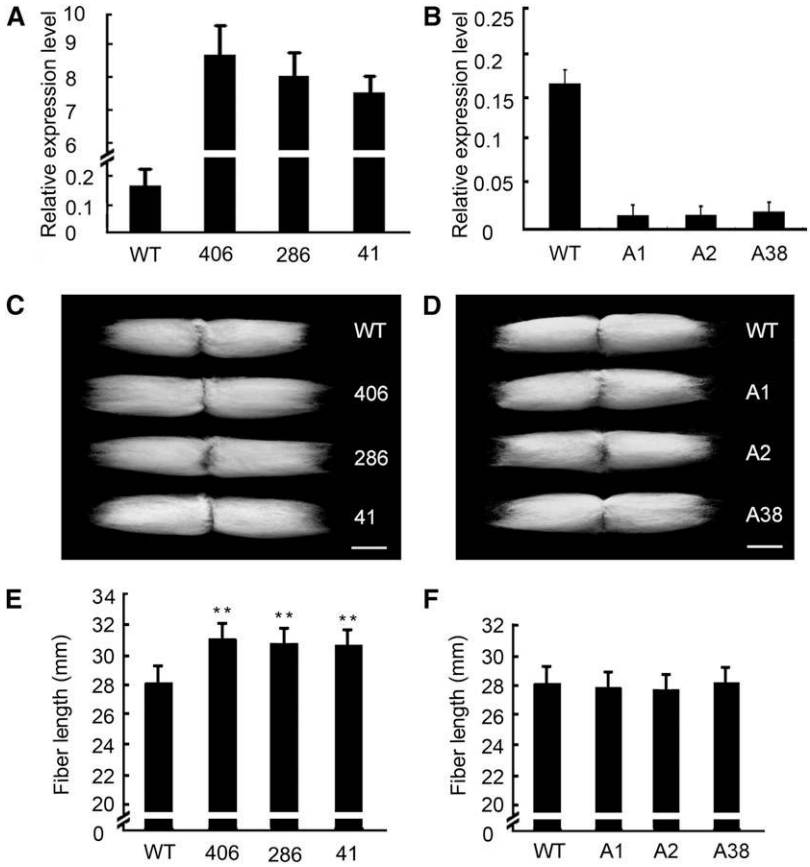

Figure 2. Phenotype Analysis of *WLIM1a*-Transgenic Cotton Fibers.

(A) and **(B)** qRT-PCR analysis of expression levels of *WLIM1a* in 12-DPA fibers of wild-type (WT), *WLIM1a*-overexpressing (lines 406, 286, and 41), and *WLIM1a*-underexpressing (lines A1, A2, and A38) plants. Error bars represent ±SE of three biological replicates.

(C) and **(D)** Images of fibers from wild-type, *WLIM1a*-overexpressing (lines 406, 286, and 41), and *WLIM1a*-underexpressing (lines A1, A2, and A38) plants. Bars = 1 cm.

(E) and **(F)** Average fiber length of wild-type, *WLIM1a*-overexpressing (lines 406, 286, and 41), and *WLIM1a*-underexpressing (lines A1, A2, and A38) plants. Error bars represent ±SE of three biological replicates (**P < 0.01, by Student's *t* test).

microscopy was also performed to view the surface of the fibers. Figure 3D shows that the arrangement of fibrils on the surface of transgenic fibers at the secondary synthesis stage was clearly different compared with the wild-type fiber. The surface of the transgenic cells looked smoother, with more uniform arrays of the fibrils aligned with each other, while grooves could be clearly seen in the surface of the control fiber cells. All these analyses revealed that the transgenic fibers possessed cell walls with different structural features.

To see if the thinner secondary wall was due to a decrease in cellulose, which constitutes more than 90% of the mature fiber mass, we measured the crystalline cellulose content and analyzed the expression levels of the cellulose synthase genes *CesA1* and *CesA2* in the cotton fibers. Despite the substantially decreased cell wall thickness, the cellulose content and the expression levels of *CesA1* and *CesA2* in the transgenic fibers were not significantly changed (see Supplemental Figure 2 online). This result indicates that a factor(s) other than cellulose biosynthesis may account for the changes in secondary wall structure.

Biosynthesis of Lignin/Lignin-Like Phenolics Is Enhanced in *WLIM1a*-Overexpressing Fibers

A previous study reported that tobacco LIM1 functions as a transcription factor to regulate lignin biosynthesis (Kawaoka et al., 2000; Kawaoka and Ebinuma, 2001); therefore, we were interested to see if WLIM1a function was also associated with lignin biosynthesis, although cotton fiber cells were previously considered to be lignin free. First, we stained cotton fibers with phloroglucinol-HCl, which stains lignin/lignin-like phenolics red. Wild-type fibers were stained faint red by phloroglucinol-HCl, compared with those soaked in buffer (Figure 4A, panels a and b), suggesting that cotton fibers of variety R15 may contain lignin/lignin-like phenolics, but at a low level. Compared with the wild-type fibers, the *WLIM1a*-overexpressing fibers stained a slightly darker color (Figure 4A, panels c to e), indicating the presence of a relatively higher amount of lignin/lignin-like phenolics. To further test for the presence of these materials in fiber cells, we applied both the Klason and thioglycolate methods to

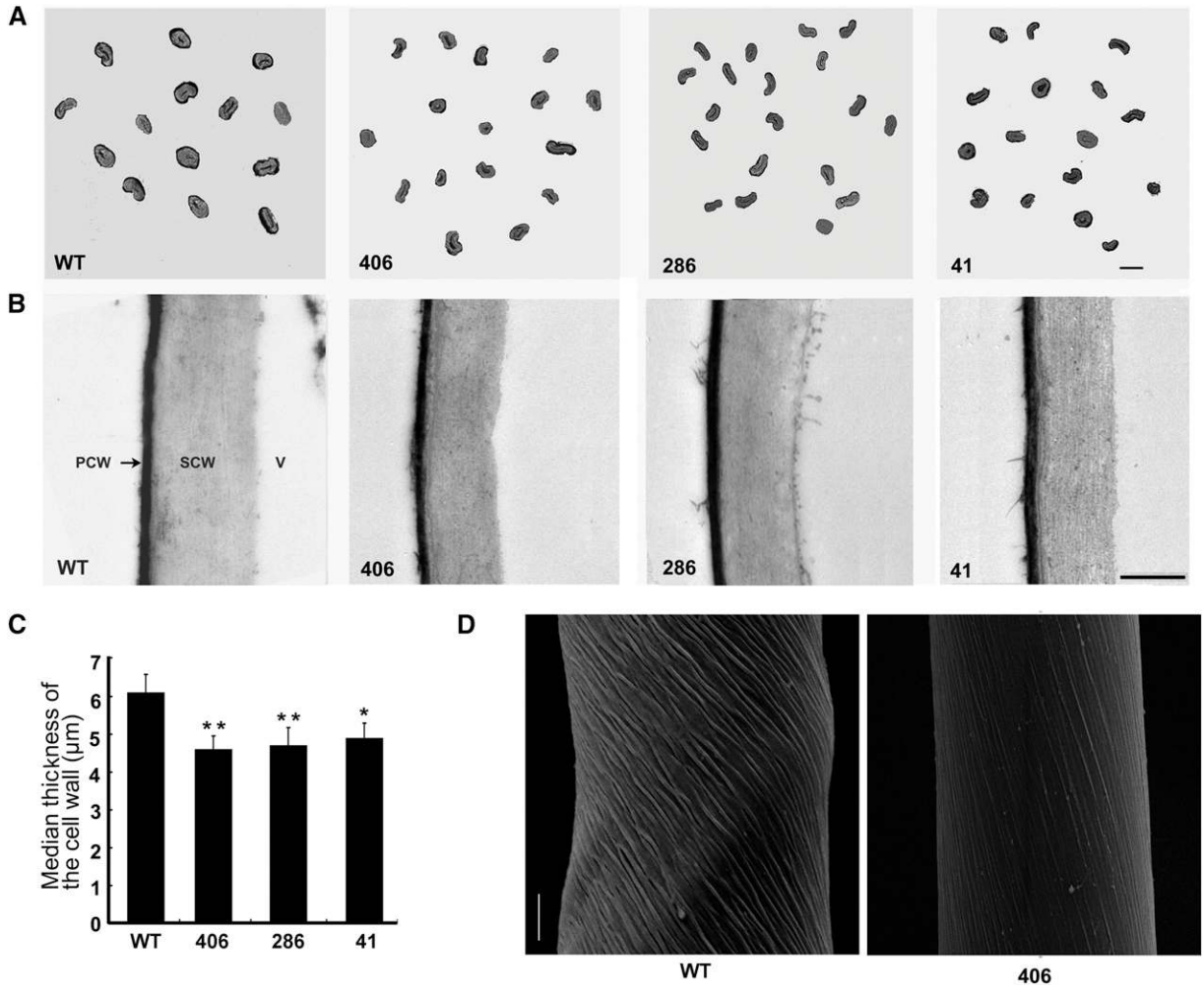

Figure 3. Cell Wall Morphology of Cotton Fibers.

(A) Cross sections of mature wild-type (WT) and *WLIM1a*-overexpressing (lines 406, 286, and 41) fibers. Bar = 20 μm.

(B) Transmission electron microscopy images of wild-type and *WLIM1a*-overexpressing (lines 406, 286, and 41) fibers. PCW, primary cell wall; SCW, secondary cell wall; V, vacuole. Bar = 5 μm.

(C) Median thickness of cell walls calculated for wild-type and *WLIM1a*-overexpressing (lines 406, 286, and 41) fibers. Values are mean ± SE (**P < 0.01 and *P < 0.05, by Student's *t* test, $n \geq 30$ per group).

(D) Scanning electron microscopy images of the surfaces of wild-type and *WLIM1a*-overexpressing (line 406) fibers. Bar = 5 μm.

measure the lignin/lignin-like phenolics in mature cotton fiber. The Klason method dissolves away polysaccharides and small soluble phenolics with sulfuric acid, leaving the insoluble lignin phenolics on the filter paper. Using this method, we clearly observed insoluble residue from wild-type and transgenic fibers (Figure 4B). The dry weight of Klason phenolics was 0.98% for the wild type and 1.54, 1.48, and 1.38% for transgenic lines 406, 286, and 41, respectively (Figure 4C). The lignin/lignin-like content measured by the thioglycolate method also showed that there were more lignin/lignin-like phenolics in

Table 1. Mean MFAs in the Secondary Cell Wall of Wild-Type and *WLIM1a*-Overexpressing Cotton Fibers

Plant	MFAs
Wild type	18.24 ± 0.53
406	16.08 ± 0.65
286	16.38 ± 0.48
41	16.62 ± 0.62

Each value is the average ± SD of about 10 measurements. 406, 286, and 41, *WLIM1a*-overexpressing lines.

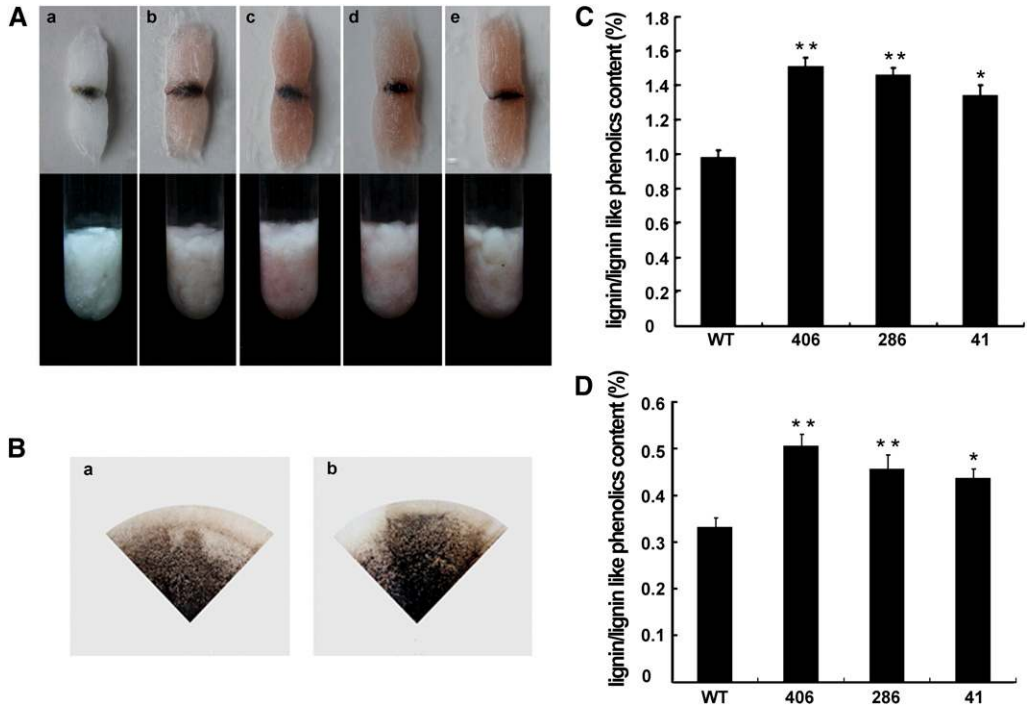

Figure 4. Evaluation of Lignin/Lignin-Like Phenolics in Wild-Type versus Transgenic Cotton Fibers.

(A) Phloroglucinol-HCl staining of wild-type and *WLIM1a*-overexpressing fibers. (a) Wild-type fibers soaked in buffer; (b) wild-type fibers stained with 2% phloroglucinol-HCl; (c) to (e) *WLIM1a*-overexpressing (lines 406, 286, and 41) fibers stained with 2% phloroglucinol-HCl.
(B) Insoluble residues remaining after Klason extraction. (a) The wild type; (b) line 406.
(C) and **(D)** Content of lignin/lignin-like phenolics estimated by Klason extraction **(C)** and thioglycolate analysis **(D)**, respectively. Error bars represent ±SE, $n \geq 30$. Asterisks indicate statistically significant differences between the wild-type (WT) and *WLIM1a*-overexpressing plants (lines 406, 286, and 41), as determined by Student's *t* test (*$P < 0.05$; **$P < 0.01$).

the *WLIM1a*-overexpressing fibers, ranging from 1.3- to 1.6-fold higher in the three transgenic lines compared with the wild-type fibers (Figure 4D). These data were consistent and reproducible with the two methods. Besides the increased amount of lignin/lignin-like phenolics in cotton fibers, we also observed ectopic deposition of lignin in peduncle phloem cells in the transgenic plants, in addition to the normal deposition in the xylem cells (see Supplemental Figure 4 online), and similar changes in lignin deposition occurred in stem phloem cells as well.

HPLC analysis of the intermediates in the phenylpropanoid biosynthesis pathway supported the results from the Klason and thioglycolate analyses. As seen in Table 2, the residues predominantly contained products of the phenylpropanoid pathway, such as caffeic acid, vanillic acid, sinapic acid, and ferulic acid in wild-type fibers, and their amounts increased in the *WLIM1a*-overexpressing cotton fibers.

WLIM1a Activates Transcription of PAL-Box Genes in the Phenylpropanoid Pathway

The increased phenolic content in *WLIM1a*-overexpressing fibers indicates that WLIM1a may play a role in the transcriptional regulation of PAL-box genes involved in phenylpropanoid biosynthesis, as previously reported for Nt-LIM1 (Kawaoka et al., 2000; Kawaoka and Ebinuma, 2001). Electrophoretic mobility shift assay (EMSA) indicated that His-tagged WLIM1a proteins indeed bound to the PAL-box, but did not bind to Oct, a binding motif for Nt-WLIM2 (Moes et al., 2013), under the same experimental conditions (see Supplemental Figure 5 online).

Table 2. HPLC Analysis of Intermediates in the Phenylpropanoid Biosynthesis Pathway

Plant	Caffeic acid	Vanillic acid	Sinapic acid	Ferulic acid
Wild type	0.74 ± 0.054	0.26 ± 0.018	0.39 ± 0.036	0.62 ± 0.057
406	1.01 ± 0.076	0.38 ± 0.026	0.67 ± 0.043	0.92 ± 0.082
286	0.98 ± 0.068	0.36 ± 0.019	0.66 ± 0.058	0.88 ± 0.084
41	0.95 ± 0.059	0.32 ± 0.034	0.58 ± 0.046	0.84 ± 0.088

Each value is the mean (mg/g dry cell walls) ± SE of three separate assays. 406, 286, and 41, *WLIM1a*-overexpressing lines.

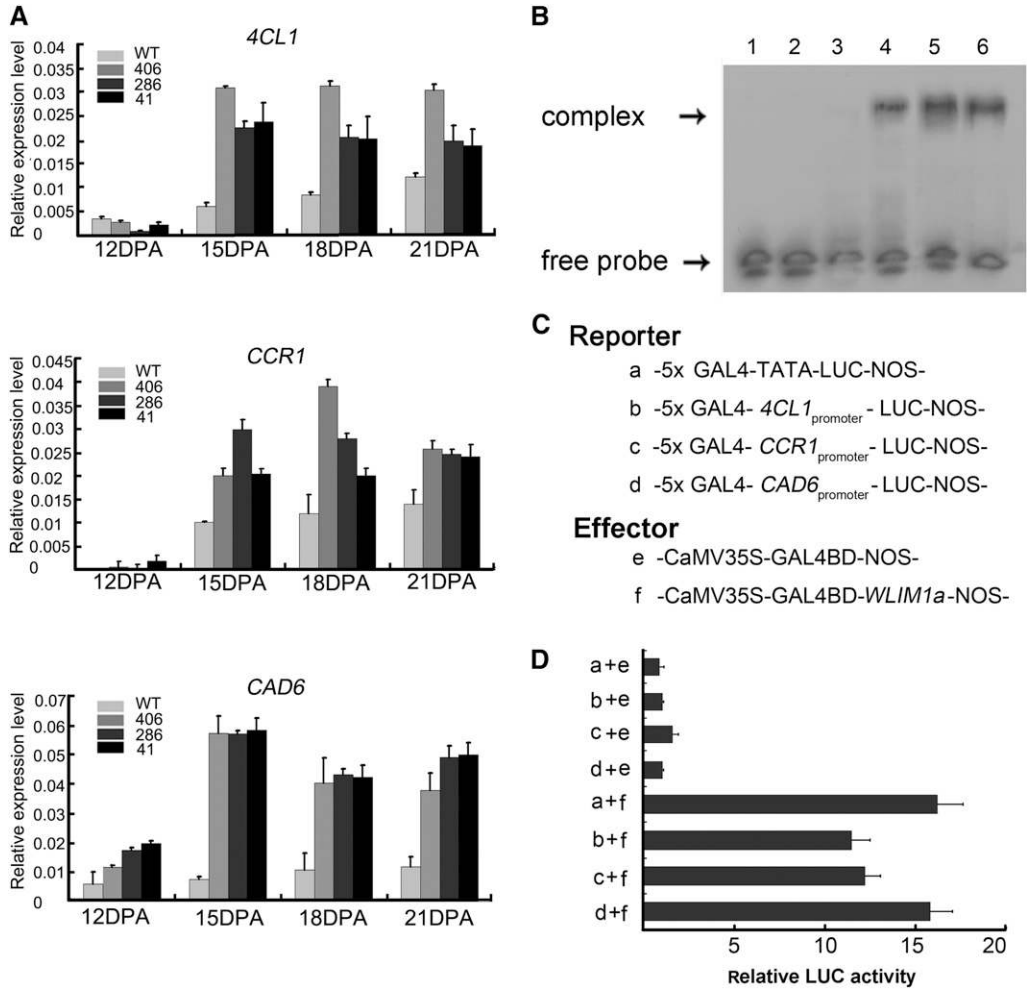

Figure 5. Assessments of Transcription Factor Activity of WLIM1a Protein.

(A) qRT-PCR analysis of the expression levels of *4CL1*, *CCR1*, and *CAD6* genes in wild-type (WT) and *WLIM1a*-overexpressing (lines 406, 286, and 41) cotton fibers. Cotton *UBI* was used as an internal control. Error bars represent ±SE of three biological replicates.

(B) EMSA of the binding of WLIM1a to the promoters of the *4CL1*, *CCR1*, and *CAD6* genes. Lanes 1 to 3, biotin-labeled probes of *4CL1*, and *CCR1* and *CAD6* promoter fragments alone; lanes 4 to 6, biotin-labeled *4CL1*, *CCR1*, and *CAD6* promoter elements incubated with WLIM1a proteins, respectively.

(C) Reporters and effectors used in the DLR assay.

(D) LUC activities measured by DLR assay. Error bars represent ±SE of three biological replicates.

To test the transcription factor activity of WLIM1a in vivo, we analyzed the expression levels of some key genes in the phenylpropanoid pathway. As expected, several genes, such as those encoding for 4-coumarate coenzyme A (CoA) ligase 1 (4CL1), cinnamoyl CoA reductase1 (CCR1), and CAD6, were expressed preferentially in the later stage of fiber development in the wild-type fibers. In the *WLIM1a*-overexpressing cotton fibers, expression of these genes was significantly induced (Figure 5A). EMSA and dual-luciferase reporter (DLR) assays were conducted to verify whether the enhanced expression of these genes was a consequence of *WLIM1a* expression. The promoters containing the PAL-box element (see Supplemental Table 1 online) of the three cotton genes (*4CL1*, *CCR1*, and *CAD6*) were cloned and used for the EMSA and DLR assays. As seen in Figure 5B, WLIM1a could bind directly to the three promoter fragments. The DLR assay was conducted according to the methods described by Ohta et al. (2001). Figures 5C and 5D show that compared with the GAL4 DNA binding domain (GAL4-BD) negative control, WLIM1a strongly activated the expression of the reporter gene; moreover, cotransfection of the effector (35S-GAL4BD-WLIM1a) and reporter (GAL4-*4CL1*pro-LUC, GAL4-*CCR1*pro-LUC, or GAL4-*CAD6*pro-LUC) also resulted in higher firefly luciferase (LUC) activity than the control.

Concurrent Improvement of Fiber Fineness and Strength in *WLIM1a*-Overexpressing Fibers

As the thickness and structure of the secondary wall are directly related to fiber fineness and strength, the two major fiber properties, we evaluated these two traits in wild-type and

transgenic fibers. We measured the micronaire value, which is used for assessing fiber fineness and maturity; a higher micronaire value usually indicates fibers with thicker cell walls (Gordon, 2007). Indeed, along with the formation of a thinner secondary wall, the micronaire values of the transgenic fibers decreased accordingly. As shown in Table 3, the micronaire units of transgenic lines 406, 286, and 41 were ~20.2, 19.1, and 19.1% lower than that of the wild type, respectively. Interestingly, we found that despite having a thinner secondary wall, the strength of the transgenic fibers increased significantly. The fiber strength values of transgenic lines 406, 286, and 41 were ~9.7, 9.0, and 7.3% higher than that of the wild type, respectively. Thus, the formation of the thinner and more compact secondary wall in WLIM1a-overexpressing fibers resulted in simultaneous improvement of fiber fineness and strength.

WLIM1a Acts as an Actin Bundler and Functions in Fiber Cell Elongation

The putative actin-related function of WLIM1a was assessed. A high-speed cosedimentation assay showed that 6×His-tagged WLIM1a cosedimented with actin filaments (Figure 6A). To verify the binding of WLIM1a to filaments actin (F-actin), we expressed recombinant 6×His-tagged WLIM1a-RFP (for red fluorescent protein) and incubated it with preassembled F-actin. Figure 6B shows that the actin filaments were decorated by WLIM1a-RFP proteins. We also calculated apparent equilibrium K_d values, as previously described by Thomas et al. (2006). The K_d value in the representative experiment (see Supplemental Figure 6 online) was 0.32, and at saturation, the stoichiometry of the interaction was 1.89:1 (WLIM1a:actin). For three such experiments, a mean dissociation constant ($K_d \pm$ SD) value of 0.42 ± 0.13 μM ($n = 3$) and a stoichiometry at saturation of 1.96 ± 0.19 mol WLIM1a bound per mol actin were calculated.

The ability of WLIM1a to bundle actin filaments was examined by low-speed cosedimentation. In the absence of WLIM1a, very few polymerized actin filaments sedimented; however, in the presence of WLIM1a, the amount of actin in the pellet increased proportionally to the WLIM1a concentration (Figure 6C). The actin bundling activity of WLIM1a was confirmed by fluorescence microscopy to visualize actin filaments stained with Alexa488-phalloidin (Figure 6D). We also tested whether the F-actin bundling activity of WLIM1a was pH or Ca^{2+} dependent like the *Arabidopsis* LIM-domain protein PLIM2c (Papuga et al., 2010) . The results indicate that WLIM1a actin bundling activity was not affected by pH or Ca^{2+} (see Supplemental Figure 7 online). This different feature of pH and Ca^{2+} dependence between PLIM2c and WLIM1a may be due to the sequence divergence at their C termini.

To characterize the cytoskeletal function of WLIM1a in vivo, we compared the F-actin structure in wild-type and transgenic fibers at the elongation stage by Alexa488-phalloidin staining. As seen in Figure 7A, both in 6- and 9-DPA cotton fibers, longitudinal or oblique actin bundles in the cortical region appeared more abundant in the transgenic fibers than in the wild-type fibers. The analysis of skewness, a statistical parameter, was conducted to quantify actin bundles (Higaki et al., 2010). Compared with that of the wild-type fiber, the skewness values were higher in transgenic fibers, indicating that the actin arrays in 6- and 9-DPA transgenic fibers were bundled to a greater extent (Figure 7B). These results indicate that WLIM1a bundles actin filaments in the living cells as it does in vitro, and this function is associated with cell elongation.

To further investigate the relevance of WLIM1a-mediated actin bundle formation to cell elongation, we also generated transgenic tobacco Bright Yellow 2 (BY2) cells overexpressing *WLIM1a*. Phenotype analysis showed that overexpression of *WLIM1a* raised the abundance of the actin bundles and led to the formation of elongated BY2 cells (see Supplemental Figure 8 online).

Cytoplasmic-Nuclear Localization of WLIM1a and Its Translocation into Nucleus in Response to H_2O_2

The subcellular distribution of WLIM1a was examined to further elucidate the mechanisms by which WLIM1a exerts its dual functions. Because of technical difficulties with the long cotton fiber cells, we used tobacco BY2 cells as a model system for this study. A plasmid containing a *WLIM1a-GFP* (for green fluorescent protein) fusion was transformed into BY2 cells. As shown in Figure 8A, panels a and d, WLIM1a-GFP fusion proteins accumulated both on the actin filaments (Figure 8A, panel b, stained with Alexa543-phalloidin) and in the nucleus (Figure 8A, panel e, stained with 4′,6-diamidino-2-phenylindole [DAPI]). The merged images (Figure 8A, panels c and f) confirmed the dual localization of WLIM1a. Although the consequence of fusing GFP to WLIM1a has not been fully characterized, the fusion proteins localized to actin bundles and were able to shuttle from the cytoplasm to the nucleus upon H_2O_2 treatment (see below), suggesting that the fusion protein is functional.

To see if the cytoplasmic WLIM1a can shuttle to the nucleus and, if so, what the trigger could be, we examined the subcellular

Table 3. Comparison of Fiber Quality Parameters between Wild-Type and *WLIM1a*-Overexpressing Plants

Plant	Fiber Length (mm)	Micronaire Units	Fiber Strength (cN/tex)	Fiber Maturity Ratio
Wild type	28.07 ± 0.85	4.7 ± 0.14	29.9 ± 0.94	1.40 ± 0.31
406	31.06 ± 0.68	3.75 ± 0.12	32.8 ± 0.65	1.39 ± 0.25
286	30.87 ± 0.59	3.8 ± 0.08	32.6 ± 0.86	1.39 ± 0.29
41	30.81 ± 0.76	3.8 ± 0.21	32.1 ± 0.78	1.40 ± 0.31

Values are mean ± SD for samples of wild-type and *WLIM1a*-overexpressing plants (lines 406, 286, and 41). The fiber length, micronaire, fiber strength, and fiber maturity ratio were measured at the National Center for Evaluation of Fiber Quality (Anyang, China). cN/tex: Centi-Newton per Tex.

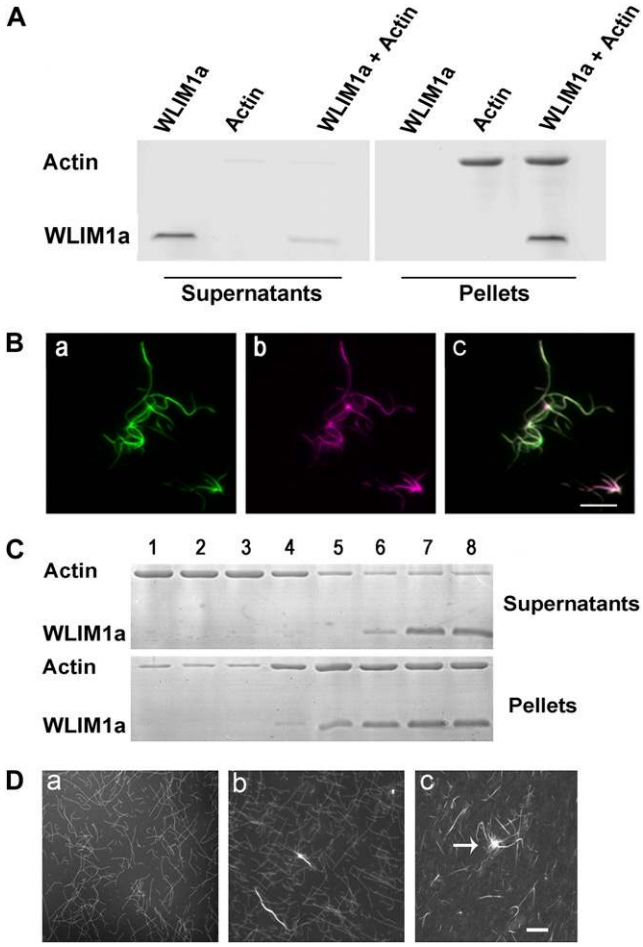

Figure 6. In Vitro Assays of Actin Binding and Bundling Activities of WLIM1a Protein.

(A) High-speed cosedimentation assay of the actin binding activity of WLIM1a. WLIM1a (3 μM) was incubated with F-actin (3 μM). The presence of WLIM1a in the pellet indicates its cosedimentation with F-actin.
(B) Images showing WLIM1a-RFP (2 μM) bound to F-actin (3 μM). (a) Preassembled F-actin labeled with Alexa488-phalloidin; (b) preassembled F-actin labeled with WLIM1a-RFP; (c) merged image of (a) and (b). Bar = 1 μm.
(C) Low-speed cosedimentation assay of the actin bundling activity of WLIM1a. The presence of WLIM1a in the pellet indicates its cosedimentation with F-actin. Lane 1, actin alone (3 μM); lanes 2 to 8, actin (3 μM) incubated with 0.2, 0.5, 1, 2, 4, 8, and 10 μM WLIM1a, respectively.
(D) Cross-linking of actin filaments visualized by fluorescence microscopy. (a) F-actin alone; (b) F-actin + 0.2 μM WLIM1a; (c) F-actin + 0.5 μM WLIM1a. The arrow indicates an actin aggregate. Bar = 1 μm.
[See online article for color version of this figure.]

distribution of WLIM1a-GFP in the absence or presence of externally applied H_2O_2, Ca^{2+}, or hormones including indole-3-acetic acid, gibberellic acid, and ethylene, which we considered as candidate triggers based on the literature. We found that WLIM1a was able to translocate from the cytosol into nucleus in response to H_2O_2 but not to Ca^{2+} or any of the hormones. As indicated in Figure 8B, panels a and d, WLIM1a-GFP was distributed within both the cytoplasm and nucleus of BY2 cells cotransformed with *WLIM1a-GFP* and *ABD2-mCherry* plasmids under normal conditions. When cells were subjected to H_2O_2 treatment, WLIM1a signals in the nucleoplasm increased from 0 to 16 min after H_2O_2 treatment, with stronger signals appeared in the nucleolus gradually (Figure 8B, panels a to c), indicating that some WLIM1a proteins translocated into the nucleus. Furthermore, a majority of the actin filaments decorated by actin binding domain2 (ABD2)-mCherry were retained in the cytosol (Figure 8B, panels e and f) after H_2O_2 treatment, indicating that the unloading of WLIM1a proteins from the F-actin bundles was not a result of a breakdown of the actin cytoskeleton. The skewness and average occupancy values of actin filaments in the cell before and after H_2O_2 treatment indicated that when WLIM1a proteins entered into the nucleus, the amount of actin bundles decreased and more, thinner actin filaments were present in the cell (see Supplemental Figures 9A and 9B online). Thus, translocation of WLIM1a into the nucleus occurred when the cells were placed in an oxidative environment. Such events were clearly revealed by time-lapse imaging, which showed that while the WLIM1a-GFP signals on actin filaments gradually disappeared, the signal in the nucleus gradually increased (see Supplemental Movie 1 online). In order to exclude the possibility that fluorescence exposure affected the translocation of WLIM1a-GFP proteins, we also performed a control experiment without application of H_2O_2. As seen in Supplemental Movie 2 online, the WLIM1a-GFP signal did not appear in the nucleus without H_2O_2 treatment over the same time period of fluorescence exposure.

It is known that a reactive oxygen species (ROS) burst occurs during the transition from elongation to secondary wall synthesis in developing fibers (see Discussion). The H_2O_2-triggered entry of WLIM1a into the nucleus of BY2 cell suggested that a similar process may occur in cotton fibers. To assess this possibility, we extracted nuclear proteins from different stages of cotton fibers, and the purity of nuclear proteins was ensured by the absence of β-actin (a marker of cytoplasmic proteins) in the protein preparations (Zhang et al., 2012) (see Supplemental Figure 10 online). Protein gel blot analysis showed that the time when WLIM1a proteins started to accumulate in the nucleus coincided with that of the ROS burst (Potikha et al., 1999). As shown in Figure 9A, the WLIM1a protein level was rather low in the nuclei of fast elongating fiber cells (6 to 12 DPA); during the transition from the elongation to secondary wall synthesis stages (15 DPA), WLIM1a proteins started to accumulate in the nucleus and increased to a higher level at the active secondary wall synthesis stage (18 to 24 DPA). qRT-PCR analysis was also conducted to examine the expression of WLIM1a-regulated genes in developing fibers, and none of the target genes tested were found to be activated in the elongating fiber cells (Figure 9B). In addition, the lignin/lignin-like phenolics were undetectable at the elongation stage (Figure 9C). To further elucidate the causal link between H_2O_2 and nuclear import of WLIM1a in the cotton fibers, we performed a protein gel blot experiment to examine whether the nuclear import of WLIM1a would be promoted or prevented after addition of H_2O_2 or ROS scavengers to ovule cultures. The results showed that when H_2O_2 was added to 9-DPA ovule cultures, WLIM1a apparently accumulated in the

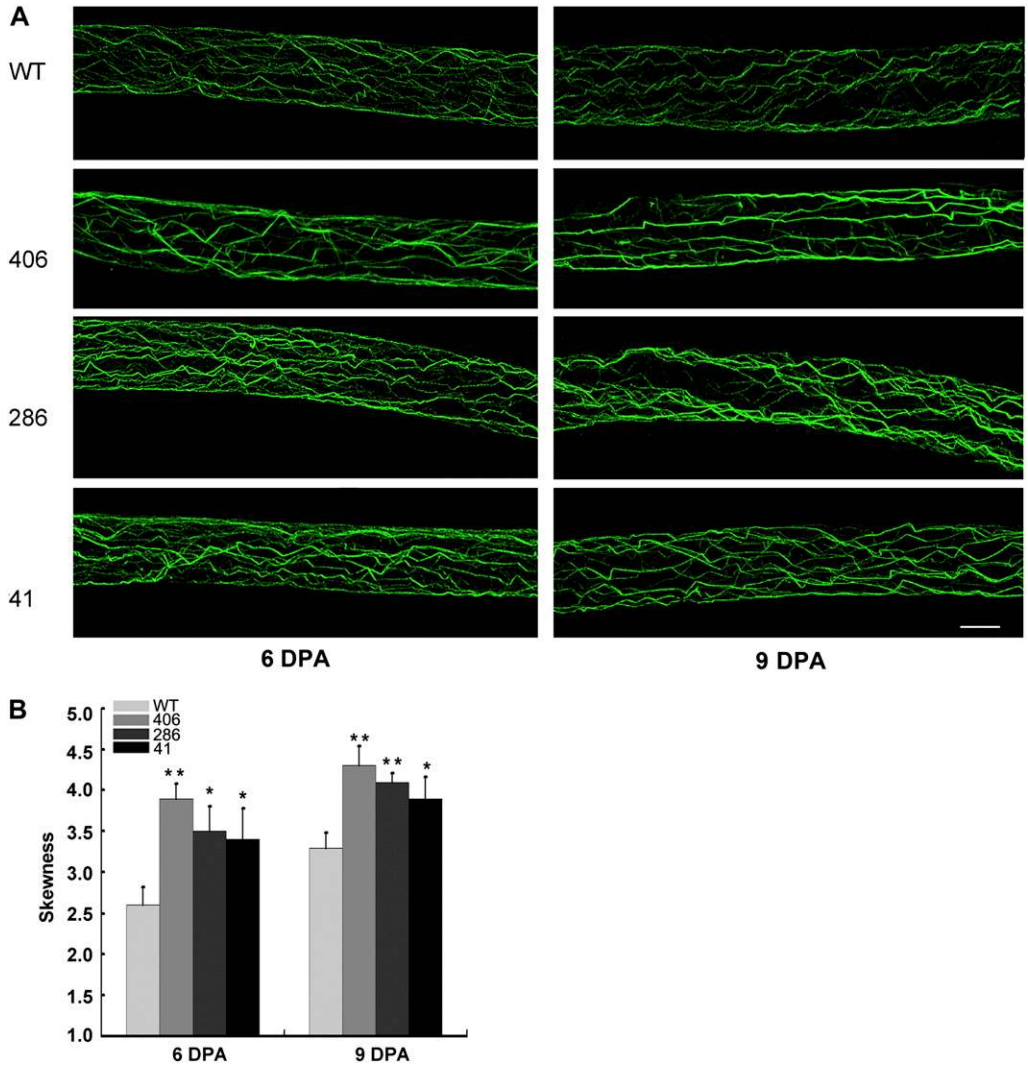

Figure 7. F-Actin Structures in Wild-Type and Transgenic Cotton Fiber Cells.

(A) F-actin organization in 6- and 9-DPA wild-type (WT) and *WLIM1a*-overexpressing (lines 406, 286, and 41) fibers. Confocal images were projected from z-series stacks. Bar = 10 μm.

(B) Values of skewness showing the extent of actin bundling in wild-type and *WLIM1a*-overexpressing (lines 406, 286, and 41) fibers. Error bars represent ±SE of three biological replicates (*P < 0.05 and **P < 0.01 and by Student's *t* test, $n \geq 30$ per group).

[See online article for color version of this figure.]

nucleus, indicating that the nuclear import of the proteins was promoted by exogenously applied H_2O_2; by contrast, when diphenyleneiodonium was added to the ovule cultures to inhibit production of ROS, WLIM1a proteins did not appear in the nuclear proteins of the fibers up to 18 DPA (Figures 9D and 9E). These results confirmed that H_2O_2 is indeed an essential trigger for the nuclear translocation of WLIM1a.

DISCUSSION

LIM-domain proteins have been identified in various plants and have been shown to have varied functions in cytoskeletal organization and transcriptional regulation. In *Arabidopsis*, all six LIM-domain proteins were found to decorate actin filaments (Papuga et al., 2010). In tobacco, LIM1 was found to be a transcriptional regulator that was able to activate the expression of a β-glucuronidase reporter gene expressed under the control of the *prxC2* promoter, and overexpression of *LIM1* led to upregulated expression of PAL-box genes *PAL*, *4CL*, and *CAD*. In addition, sunflower LIM1 was shown to bind to microtubules and has a nuclear function in interphase cells (Brière et al., 2003). Recently, it was reported the Nt-WLIM2 has dual functions in actin bundling and transcriptional activation of the histone gene, and it shuttles to the nucleus in response to cytoskeletal remodeling (Moes et al., 2013). In our study, both in vitro and in vivo data showed that WLIM1a has dual functions in

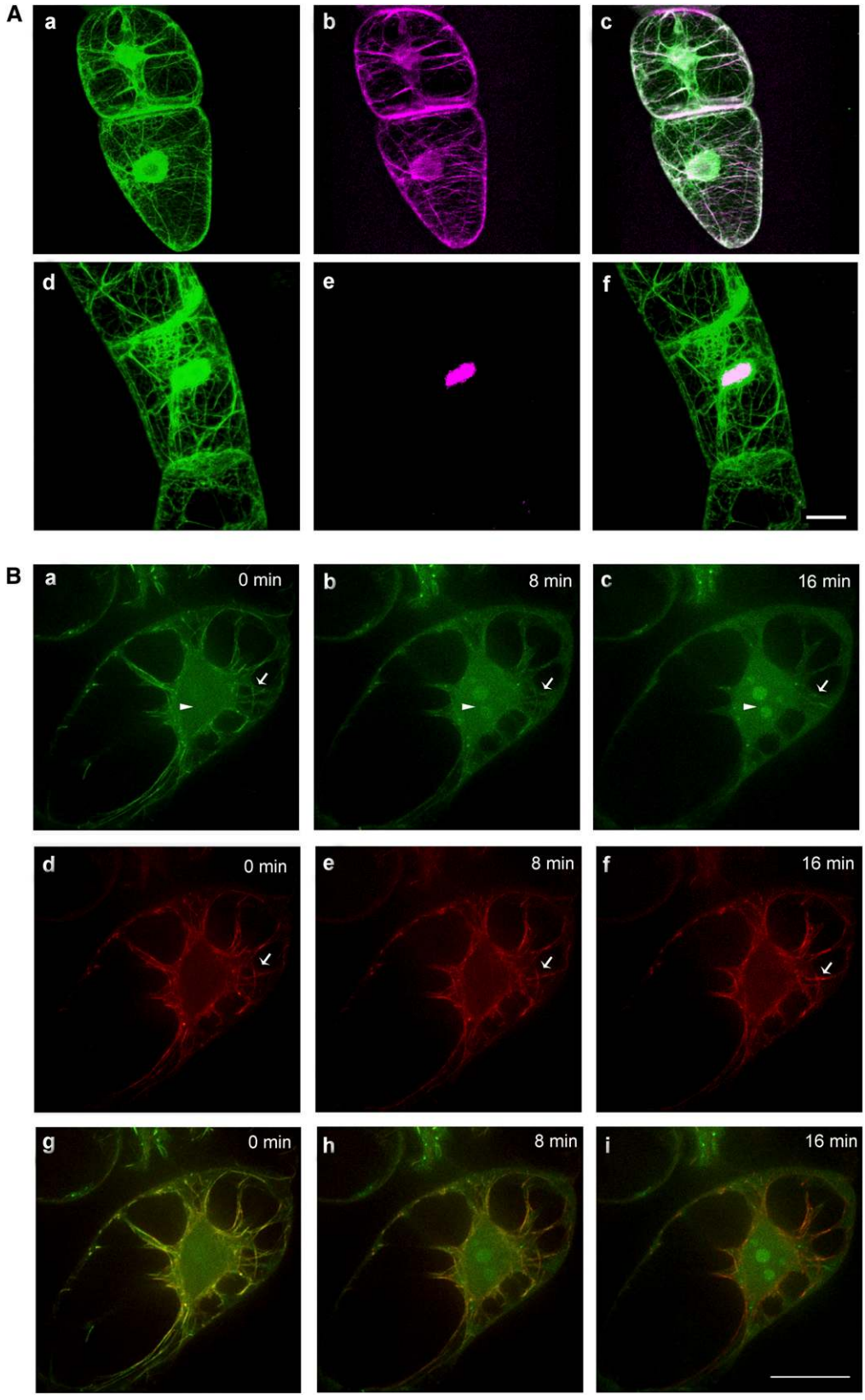

Figure 8. Subcellular Localization of WLIM1a and Its Translocation from the Cytosol into the Nucleus in Tobacco BY2 Cells.

(A) Subcellular localization of WLIM1a-GFP in BY2 cells. (a) and (d) Green fluorescence of WLIM1a-GFP fusion proteins; (b) Alexa543-phalloidin stained actin filaments in (a); (e) DAPI-stained nucleus in (d); (c) and (f) merged images. Bar = 20 μm.

actin bundling and transcriptional activation of PAL-box genes involved in the biosynthesis of lignin/lignin-like phenolics and that cytoplasmic WLIM1a could translocate into the nucleus, which is triggered by H_2O_2. Taken together, these studies imply a complicate spectrum of LIM functions in plants. On one hand, LIM cytoskeletal functions are linked with both actin cytoskeleton and microtubules; on the other hand, their transcription factor functions target different genes. Moreover, their cytoplasmic-nucleus movements can be triggered by different stimuli. Thus, it seems that the cellular roles of LIM protein family are more multifaceted than might be expected.

WLIM1a Contributes to Fiber Elongation through Its Actin Bundling Activity

In plant cells, actin bundles serve as tracks for intracellular transport. It has been shown that actin bundles are required for proper cell elongation and morphogenesis (Hussey et al., 2006; Staiger and Blanchoin, 2006). Cotton fibers are highly specialized single cells. During the fast elongation stage, cotton fibers undergo enormous growth and increase their length 1000 to 3000 times the diameter of the cell (Meinert and Delmer, 1977), a process that requires highly active cellular transport. To cope with this requirement, F-actin filaments must be actively assembled to transport the large amounts of cell wall and membrane components required for cell expansion. In this study, we observed that *WLIM1a* is expressed predominantly in fiber cells, and its overexpression led to increased cell length associated with the formation of more abundant actin filament bundles. Such a relationship between actin bundles and cell length was also observed in *WLIM1a*-transgenic BY2 cells. Our results suggest that WLIM1a contributes to rapid fiber elongation via its function in actin filament bundling. In agreement with our data, lily LIM1 has been found to participate in the regulation of actin filament organization and dynamics during pollen tube elongation (Wang et al., 2008).

WLIM1a Functions in Secondary Wall Formation and May Mediate Crosstalk between the Cytoplasm and Nucleus in Developing Cotton Fibers

In our study, we found that WLIM1a functions as a transcription factor to activate the expression of PAL-box genes in the phenylpropanoid pathway, and overexpression of *WLIM1a* promoted the biosynthesis of the lignin/lignin-like phenolics in transgenic fibers. Cell wall structure analyses by transmission electron microscopy and x-ray diffraction revealed a thinner cell wall with smaller microfibrilar angles. Based on the function of lignin in cross-linking cellulose microfibrils, we assume that the increase in lignin/lignin-like phenolics in the transgenic fiber cells may enhance the cohesion of the cellulose microfibrils, which were not altered in terms of quantity, thus leading to the formation of a thinner and more compact cell wall with improved fiber fineness and strength.

In our previous study, we found that the presence of higher amounts of actin bundles by downregulation of actin depolymerizing factor led to the formation of transgenic fiber cells with increased strength and thickness (Wang et al., 2009). Here, we observed that overexpression of *WLIM1a* resulted in increased production of both actin bundles and lignin/lignin-like phenolics in cotton fibers. Although we cannot rule out the possibility that the presence of more actin bundles had an effect on the strength-related wall structure of the *WLIM1a*-overexpressing fibers, the formation of thinner and more compacted secondary walls in these cells should be attributed to the enhanced biosynthesis of lignin/lignin-like phenolics.

In cotton fibers, an ROS burst occurs during the transition from the elongation to the secondary wall synthesis stages, and this ROS burst is required for the onset of secondary wall synthesis (Potikha et al., 1999; Hovav et al., 2008). *WLIM1a* is expressed mainly during the elongation and the secondary wall synthesis stages. When the fiber is rapidly elongating, WLIM1a may act as an actin bundling protein and contribute mainly to active intracellular transportation. Once fiber elongation is arrested when the ROS burst occurs, WLIM1a may respond to the high ROS levels and enter into the nucleus, where it serves as a transcription factor to activate the expression of the genes in the phenylpropanoid biosynthesis pathway. Thus, WLIM1a may play an important role in the crosstalk between the processes of cell elongation and secondary wall synthesis in developing cotton fibers.

Lignin/Lignin-Like Phenolics May Represent a Determinant of Fiber Properties

Although it has been widely accepted that cotton fiber contains no lignin, several recent studies raised the possibility that lignin/lignin-like phenolics are actually synthesized in cotton fiber cells (Gou et al., 2007; Al-Ghazi et al., 2009; Fan et al., 2009). In this study, our results support the presence of lignin/lignin-like phenolics in cotton fibers based on the following observations. First, using two different lignin measurement methods, lignin/lignin-like phenolics were detected in wild-type fiber cells, and HPLC analysis identified the key intermediates of the phenylpropanoid biosynthesis pathway. Second, real-time PCR analysis detected relatively high levels of expression of the PAL-box genes at the secondary wall synthesis stage in wild-type fibers. Third, overexpression of *WLIM1a* enhanced the expression of

Figure 8. (continued).

(B) Time-lapse images showing the translocation of WLIM1a-GFP fusion proteins from the cytosol into the nucleus. WLIM1a proteins were translocated from the cytosol into the nucleus after treatment with H_2O_2 in BY2 cells expressing WLIM1a-GFP and ABD2-mCherry. (a) to (c) WLIM1a-GFP signal patterns at 0, 8, and 16 min after treatment with H_2O_2 (1 mM), respectively. (d) to (f) Actin filaments decorated by ABD2-mCherry under the same conditions as (a) to (c). (g) to (i) Merged images. See Supplemental Movie 1 online for the entire series. The arrows and arrowheads indicate actin filaments and nuclei, respectively. Bar = 20 μm.

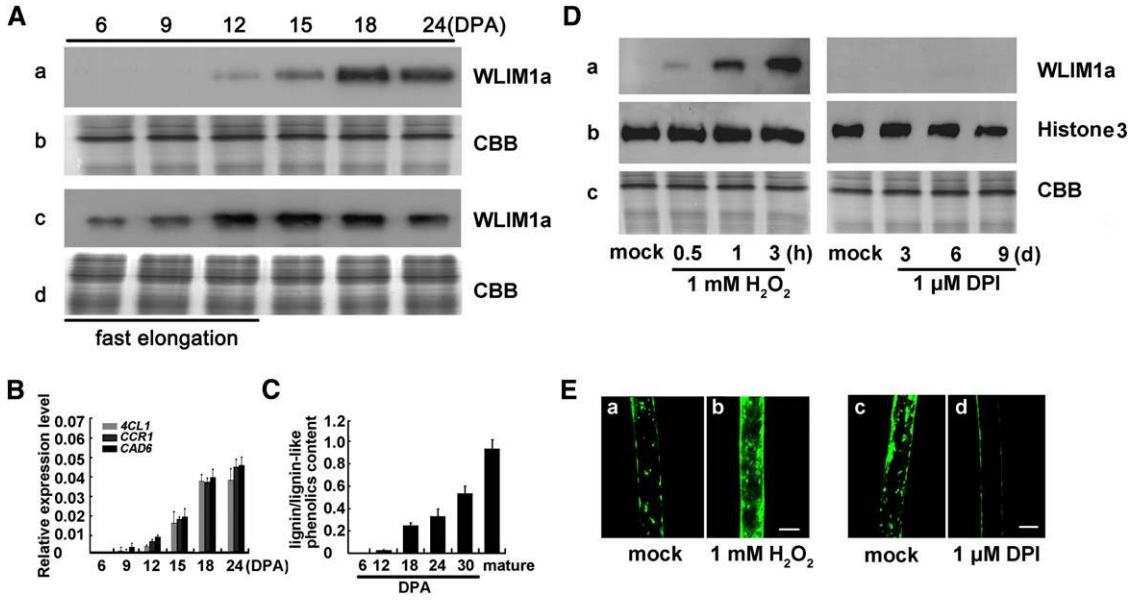

Figure 9. Analysis of the Link between ROS and Nuclear Translocation of WLIM1a in Cotton Fibers.

(A) Protein gel blot analysis of WLIM1a in nuclear and total proteins in developing fiber cells. (a) and (c) WLIM1a in nuclear and total proteins, respectively. (b) and (d) CBB, Coomassie blue staining of the gel to show equal loading of nuclear and total proteins, respectively.

(B) qRT-PCR analysis of the expression of *4CL1*, *CCR1*, and *CAD6* genes in developing fiber cells. The cotton *UBI* gene was used as an internal control. Error bars represent ±SE of three biological replicates.

(C) Thioglycolate analysis on the content of lignin/lignin-like phenolics in developing and mature fiber cells. Error bars represent ± SE of three biological replicates.

(D) Analysis of the translocation of WLIM1a into the nucleus in response to exogenous addition of H_2O_2 (left panels) and diphenyleneiodonium (DPI; right panels). (a) and (b) Protein gel blot analysis of WLIM1a and Histone 3; (c) CBB, Coomassie blue staining of the gel to show equal loading of nuclear proteins. The 9-DPA fibers were treated without or with H_2O_2 (1 mM) for 0.5, 1, and 3 h or with diphenyleneiodonium (1 μM) for 3, 6, and 9 d, respectively. Nuclear proteins were then extracted.

(E) Fluorescence analysis of 2',7'-dichlorodihydro-fluorescein diacetate-stained ROS in cotton fibers after treatment with H_2O_2 or diphenyleneiodonium. (a) 9-DPA fiber; (b) 9-DPA fiber treated with H_2O_2 (1 mM) for 3 h; (c) 15-DPA fibers; (d) 9-DPA fiber treated with 1 μM diphenyleneiodonium for 6 d. Bars = 20 μm. [See online article for color version of this figure.]

the PAL-box genes and led to the production of higher amounts of lignin/lignin-like phenolics in transgenic fiber cells, which affected the development of fiber properties. Based on these experimental data, it seems reasonable to believe that lignin/lignin-like phenolic polymers are constituents of the secondary cell walls of cotton fiber cells. The earlier conclusions about the absence of lignin/lignin-like may be attributable to the low content of lignin in fiber cells and the technical limitation for detection of such low percentages of this substance.

According to our results as well as those of other studies (Gou et al., 2007; Al-Ghazi et al., 2009; Fan et al., 2009; Wang et al., 2012), it is possible that lignin/lignin-like phenolics is a determinant of cotton fiber quality.

Application Potential of the *WLIM1a* Gene

Higher quality natural fibers are highly desirable for the current textile market to meet demands based on the increasing standard of living and advanced textile techniques. Because of the frequently observed negative correlation between fiber fineness and strength, the concurrent improvement of the two traits has been a bottleneck problem in cotton breeding. We found that a slight increase in *WLIM1a* gene expression could enhance the expression of PAL-box genes and augment the lignin/lignin-like phenolic content, which led to a favorable improvement in both fiber fineness and strength. Thus, our results provide a clue for concurrent improvement of fiber quality properties via genetic manipulation of *WLIM1a* or other genes involved in the biosynthesis of lignin/lignin-like phenolics.

Finally, two points should be considered regarding the biosynthesis of lignin/lignin-like phenolics in fiber cells and in term of its application: (1) Because of the technical limitation in determining the polymer length of lignin/lignin-like phenolics, we cannot rule out the possibility that the lignin/lignin-like phenolics we described here are different from the lignin phenolics in the secondary walls of other plant cells in characteristics including polymerization status, etc. Further study is required to verify the biochemical nature of the cotton fiber lignin/lignin-like phenolics. (2) Although an increase in the lignin/lignin-like phenolics could improve fiber fineness and strength, it might also increase the rigidity of fiber cells, which is unfavorable for spinnability of the fibers. Thus, the biosynthesis of lignin/lignin-like phenolics must be modulated to an optimal level in cotton fibers.

METHODS

Plant Materials and Growth Conditions

The wild-type cotton variety R15 (*Gossypium hirsutum*) and *WLIM1a* transgenic cotton plants (T3 generation) were used in this study. The cotton plants were cultivated in the field under standard conditions. Flowers were tagged on the day of anthesis. Cotton bolls were harvested at 0, 3, 6, 9, 12, 15, 18, 21, 24, 27, 30, and 35 DPA, respectively. Ovules were excised from the bolls, and fibers were scraped from the ovules. All collected materials were immediately frozen in liquid nitrogen and stored at −80°C before use.

For ovule culture, the bolls were collected at 2 DPA, surface sterilized with 95% (v/v) ethanol for 5 s, then flamed briefly to remove the ethanol residue. The seeds were cultured on BT medium (Beasley and Ting, 1973) containing 0.5 μM indole-3-acetic acid, 0.5 μM gibberellic acid, and 200 mg/mL of cefotaxime in the dark at 30°C without agitation.

Cloning of *WLIM1a* cDNA

Total RNA (2 μg) from 12-DPA cotton fibers was used in the RACE experiments using a BD SMART RACE kit (Clontech, TAKARA BIO Group). The primers (see Supplemental Table 2 online) used in 5′ RACE were designed based on the EST sequence (GenBank accession number ES847697) obtained from the National Center for Biotechnology Information. The full-length cDNA (GenBank accession number JX648310) was obtained by PCR. Open reading frame (ORF) and motif analyses were performed with National Center for Biotechnology Information BLAST and DNAMAN version 6.0.

Phylogenetic Analysis

The protein sequences were aligned using the ClustalX program version 2.1 (Larkin et al., 2007) with the default settings (see Supplemental Data Set 1 online), and the neighbor-joining method was used to produce an unrooted phylogenetic tree by the MEGA program version 5.1 (Tamura et al., 2007). Bootstrap test with 1000 replicates was used to evaluate the consistency of the analysis.

RNA Extraction and qRT-PCR

Total RNA from cotton roots, leaves, stems, flowers, cotyledons, ovules, anthers, petals, and fibers was extracted according to the ultracentrifugation method (John and Crow, 1992). For cDNA synthesis, 2 μg of total RNA from different tissues was used for reverse transcription with Moloney murine leukemia virus reverse transcriptase according to the manufacturer's recommendations (Promega). The qRT-PCR assays were performed using SYBR Green real-time PCR master mix (Toyobo) and a DNA Engine Opticon 2 real-time PCR detection system (MJ Research). All reactions were performed in triplicate. The primers used in RT/qRT-PCR are shown in Supplemental Table 2 online.

Plasmid Construction and Protein Expression

To construct plasmids harboring *35S-WLIM1a*, *35S-WLIM1a-GFP*, and *35S-WLIM1a-mCherry*, *WLIM1a* cDNA was amplified using gene-specific primers and cloned into the plant expression vectors pPZP111 (Hajdukiewicz et al., 1994) (predigested with *Bam*HI and *Sac*I), pPZP111-GFP (predigested with *Bam*HI and *Sac*II), and pCAMBIA1301-mCherry (predigested with *Bam*HI and *Sac*I) (Invitrogen), respectively. The *WLIM1a* ORF was inserted into pPZP111 between *Bam*HI and *Sac*I sites in the antisense orientation to generate antisense plasmid. The recombinant plasmids were introduced into cotton or BY2 cells by *Agrobacterium tumefaciens*–mediated transformation (Horsch et al., 1985).

The cDNA fragment containing *WLIM1a* ORF was digested with *Bam*HI and *Sal*I and cloned into the bacterial expression vector PET-28a (Novagen/Merck). The recombinant proteins were expressed in *Escherichia coli* strain BL21 (DE3). His-tagged WLIM1a proteins were purified using nickel-nitrilotriacetic acid resin following procedures described by the manufacturer (Qiagen).

His-tagged WLIM1a-RFP recombinant proteins were expressed in *E. coli* and purified following similar procedures as described above. All primers and enzyme sites used in plasmid construction are described in Supplemental Table 2 online.

High- and Low-Speed Cosedimentation Assays

High- and low-speed cosedimentation assays were conducted according to Wu et al. (2010). Rabbit muscle actin proteins were dissolved in A-buffer (5 mM Tris-HCl, pH 8.0, 0.2 mM $CaCl_2$, 0.2 mM Na_2ATP, and 0.5 mM DTT). All solutions were preclarified at 200,000*g* for 60 min. Mg-ATP-actin was prepared by incubation of Ca-ATP-actin on ice with 1 mM EGTA and 0.1 mM $MgCl_2$ for 2 min and used immediately. Actin (3 μM) was incubated at 22°C for 60 min either alone or with 3 μM WLIM1a in 1× KMEI buffer (10× stock: 500 mM KCl, 10 mM $MgCl_2$, 10 mM EGTA, and 100 mM imidazole, pH 7.0). For high-speed cosedimentation assay, the samples were centrifuged at 200,000*g* for 60 min in an Optima TLX ultracentrifuge (Beckman) at 4°C; for low-speed cosedimentation assay, the samples were centrifuged at 13,500*g* for 30 min at 4°C. The proteins in the supernatants and pellets were separated by SDS-PAGE and visualized with Coomassie Brilliant BlueR 250.

To determine the WLIM1a-actin K_d, WLIM1a in increasing concentrations (0.1 to 10 μM) was incubated with 3 μM preassembled Mg-ATP-actin in 1× KMEI buffer for 60 min at 22°C. Samples were cosedimented and analyzed as described above, and the amount of WLIM1a in the pellets or supernatants was quantified using Glyko Bandscan version 5.0. The moles of bound WLIM1a proteins per mole of actin subunits at saturation and the K_d value were determined by fitting the data of bound protein versus free protein to a hyperbolic function with GraphPad Prism version 4.03 software. Low-speed cosedimentation was conducted to determine the effects of Ca^{2+} and pH on the actin bundling activity of WLIM1a. The buffers containing various concentration of Ca^{2+} or different pH were prepared as described by Papuga et al. (2010). The reaction buffers were supplemented with increasing amounts of Ca^{2+} (from 10 nM to 10 mM), and the pH was adjusted to values ranging from 6.2 to 8.0. After sedimentation, the proteins were examined by SDS-PAGE.

Visualization of Actin Filaments by Fluorescence Microscopy

F-actin (3 μM) was incubated with WLIM1a and WLIM1a-RFP at the indicated concentrations at room temperature for 30 min and then labeled with 4 μM Alexa488-phalloidin (Invitrogen). Actin filaments were subsequently diluted to a final concentration of 10 nM in fluorescence buffer (10 mM imidazole, pH 7.0, 50 mM KCl, 2 mM $MgCl_2$, 1 mM EGTA, 100 mM DTT, 100 μg/mL Glc oxidase, 15 mg/mL Glc, 20 mg/mL catalase, and 0.5% methylcellulose) as described by Michelot et al. (2005). The diluted samples were visualized using a 1.0 Iris ×40 oil immersion lens mounted on an Olympus BX51 microscope. For Actin-Alexa488-phalloidin observation, a B-4 filter (Olympus) was used to generate blue fluorescence, and for the RFP-WLIM1a observation, a G-2 filter (Olympus) was used to generate green fluorescence. Images were collected with a Leica Spot Pursuite charge-coupled device camera using SPOT version 4.7 software.

Fluorescent Staining and Confocal Laser Scanning Microscopy

Actin filament staining in cotton fibers was performed mainly according to J. Wang et al. (2010). Cultured ovules with fibers attached were stained in PBS, pH 7.0, containing 0.066 μM Alexa488-phalloidin (Molecular

Probes), 0.1 M PIPES, pH 6.9, 0.05% (v/v) Triton X-100, 1 mM $MgCl_2$, 3 mM DTT, 0.3 mM phenylmethylsulfonyl fluoride (PMSF), 5 mM EGTA, and 0.25% glutaraldehyde.

Actin microfilament staining in BY2 cells was performed as described by Traas et al. (1987). Briefly, 1 volume of a 5-d-old BY2 subculture was incubated for 15 min in 1 volume of staining buffer (50 mM PIPES, 50 mM EGTA, 20 mM $MgCl_2$, 5% DMSO, and 0.01% Nonidet P-40, pH 6.9), and then supplemented with 1 μM Alexa543-phalloidin (Molecular Probes) and DAPI (1 mg/mL) if needed.

Cells were examined under a confocal laser microscope (Leica TCS SP5; Leica Microsystems) in multitrack mode (at 0.75-μm steps with two-line averaging and one-frame averaging). Excitation wavelengths and emission filters were as follows: 405 nm/band-pass 420 to 480 nm for DAPI, 488 nm/band-pass 505 to 530 nm for GFP and Alexa-Fluor 488, and 543 nm/long-pass 560 to 600 nm for Alexa Fluor 543.

Quantitative Analysis of Actin Filament Bundling in Cotton Fibers

Skewness analysis was performed to quantify the extent of actin bundling in cotton fibers according to a previously described method (Higaki et al., 2010; Henty et al., 2011). The z-series stacks of all optical sections were filtered using Gaussian blur to reduce background noise and then skeletonization was assessed with the procedure of ThinLine (a JAVA plug-in procedure; Higaki et al., 2010). The actin filament pixels were collected into a single image using maximum intensity projections, and the skewness values were calculated.

Analyses of Cell Wall Structure and Fiber Properties

Paraffin sections of mature cotton fibers were used for statistical analysis of cell wall thickness. Mature cotton fibers were fixed in FAA (37% formaldehyde/glacial acetic acid/50% ethanol, 5:6:89, by volume) for 12 h at 25°C. After gradient dehydration and infiltration, the samples were embedded in paraffin and 6-μm sections were generated. The slices were examined and photos were taken under a microscope (Olympus BX 51). The surface of mature fibers was examined by cold-field scanning electron microscopy after dehydration and platinum spraying. The mature and 30-DPA cotton fibers were analyzed by transmission electron microscopy according to a previous report (Wang et al., 2009). X-ray diffraction was performed using an X' Pert PRO MPD diffractometer, following the method described previously (Stuart and Evans, 1994; Cave, 1997). The 2θ was set as 22.6°, the cotton fibers were irradiated vertically by the x-ray, and then the specimen were rotated vertically from 0° to 360°. The reflection curve was generated according to the record of the reflection. The model is $y = a+b\cdot\exp[-(x-\mu)^2/2\sigma^2]$. Here, a is constant background, μ is the center of the peak, σ is the half-width at inflection point, and b indicates the height of the curve above constant background. The T value was estimated as 2σ. Microfibril angle (MFA) value was estimated from the equation MFA = 0.6T.

The length, strength, micronaire values, and maturity of matured fibers were measured at the National Center for Evaluation of Fiber Quality (Anyang, China).

EMSA

EMSAs were performed using biotin-labeled probes and the Lightshift Chemiluminescent EMSA kit (Pierce). The binding reaction was performed in a 20-μL reaction mixture containing the indicated LIM proteins, 20 nmol of synthetic biotin-labeled DNA probe (conserved PAL-box; Oct motif; *4CL1*, *CCR1*, and *CAD6* promoter fragments containing PAL-box, as described in Supplemental Table 2 online), and 50 ng poly(dI-dC). The reaction mixtures were incubated at room temperature for 30 min and then the samples were separated on a 6% native polyacrylamide gel in 0.5× TBE buffer (45 mM Tris-borate, 1 mM EDTA, pH 8.0). Electrophoresis was performed at 15 V/cm in 0.5× TBE buffer. For the competition assay, appropriate amounts of unlabeled PAL-motif DNA fragments were used as competitors and were added to the reaction prior to the addition of the proteins. The labeled probes were transferred to positively charged nylon membrane and detected using the chemiluminescent nucleic acid detection module provided with the kit.

Protoplast Assay of Transcription Factor Activity

The DLR assay was performed according to Ohta et al. (2001). The GAL4 reporter plasmid contains the *LUC* gene, driven by the minimal TATA region of the 35S promoter with five GAL4 binding elements upstream. The reporter plasmids were constructed by inserting *4CL1*, *CCR1*, and *CAD6* promoters after the GAL4 binding elements, respectively. The *Renilla* luciferase gene driven by the 35S promoter was used as an internal control. For construction of the effector plasmid, the coding region of *WLIM1a* was cloned into expression vector pRT-BD to generate *35S-GAL4BD-WLIM1a* plasmid.

Isolation and transfection of *Arabidopsis thaliana* protoplasts were performed based on the protocol provided by He et al. (2007). Six micrograms of reporter construct, 6 μg of effector construct, and 0.5 μg of internal control were used for each polyethylene glycol cotransfection. After 16 h of culturing, luciferase assays were performed with the Promega DLR assay system and values were measured with the GloMax 20-20 luminometer.

Measurements of Cellulose Content in Cotton Fibers

The cotton fibers were cut, and the middle parts (1.5 cm) were used for determination of the cellulose content. The cut fibers (10 mg) of wild-type and transgenic cotton fibers were used to count the fiber numbers with ~30 repeats for each line. As no significant difference in the fiber numbers was observed between the wild-type and transgenic fibers, the aliquots of the cut fibers were used. Alcohol-insoluble cell wall residues were prepared from cotton fibers as previously described (Harholt et al., 2006). Two milligrams of destarched alcohol-insoluble cell wall residue sample was hydrolyzed in 2 M trifluoroacetic acid at 121°C for 90 min and then centrifuged to collect the supernatants. The crystalline cellulose content was analyzed by hydrolyzing the remains of trifluoroacetic acid treatment with Updegraff reagent (acetic acid:nitric acid:water, 8:1:2, by volume) at 100°C for 30 min. After treating the pellets with 72% sulfuric acid, the content was quantified via an anthrone assay (Updegraff, 1969).

Determination of Lignin/Lignin-Like Phenolics in Cotton Fibers

For detection of lignin/lignin-like phenolics in cotton fibers, the samples were stained for 30 min with 2% phloroglucinol in 6 M HCl. The Klason and thioglycolate methods were used to determine the amounts of lignin/lignin-like phenolics (Hatfield and Fukushima, 2005; Fan et al., 2009). The mature and dry cotton fibers were used to generate Klason lignin. The dried cotton fibers were ground into a fine powder, extracted four times in methanol, and dried. Then, 2 g of the extract was mixed with 5 mL of 72% sulfuric acid at 30°C and hydrolyzed for 60 min. The hydrolysate was diluted to 4% sulfur by the addition of water and then autoclaved. The residue was filtered through a dry glass filter (W1). The sample with the filter was washed with deionized water, dried at 60°C, and then weighed (W2). The samples were burned in a muffle furnace and the ashes were collected (W3). The lignin content was measured and expressed as a percentage of the original weight of cell wall residues. The concentration of lignin-like phenolics = (W2-W1-W3)/2 × 100%.

Cotton fiber powder (100 mg) was used for lignin measurement using the thioglycolate method (Müse et al., 1997). Samples were placed in a plastic tube with 5 mL of 2 M HCl and 1.5 mL of thioglycolic acid for 4 h at 98°C with gentle shaking. After centrifugation (15,100*g*, 15 min), the

pellets were washed three times with distilled water and the thioglycolate lignin phenolics were extracted with 5 mL of 0.5 M NaOH for 10 to 12 h with shaking. After extraction four times, the supernatants were obtained and acidified with 7.5 mL of 12 M HCl. Lignin-othioglycolic acid was allowed to precipitate for 4 h at 4°C and then recovered by centrifugation (15,100*g*, 20 min) and dissolved in 10 mL of 0.5 M NaOH. The absorbance was detected against a 0.5 M NaOH blank at 280 nm using a Shimadzu UV-1750 spectrophotometer. Three replicates were included in these experiments. At least 12 samples were used for each replicate.

HPLC Analysis

HPLC analysis of intermediates in phenylpropanoid biosynthesis pathway was mainly performed according to a previous report (Müse et al., 1997). Cotton fiber residues (200 mg) extracted by the thioglycolate method were saponified with 2 mL of 4 M NaOH for 24 h at 35°C. To acidify the samples, 0.76 mL of 12 M HCl was added, followed by addition of 7.4 mL of 0.1 M phosphate buffer, pH 2.1. After filtration, the solution was extracted three times in a tube with an equal volume of CH_2Cl_2 and the organic phase was retained. The combined organic phases were dried with a rotary evaporator, and all of the residue was dissolved in 1 mL of methanol. Sample analysis was performed using HPLC spectrometry on a 2010 eV LC/UV spectroscopy instrument (Shimadzu). The mobile phase solvents were composed of 1% acetic acid in water (solvent A) and 100% acetonitrile (solvent B). The column was treated with a gradient solvent system that was designed to separate the metabolites. The ratios of solvent A to B were 90:10 (0 to 5 min), 88:12 (5 to 10 min), 80:20 (10 to 20 min), 75:25 (20 to 30 min), 65:35 (30 to 35 min), 60:40 (35 to 40 min), and 50:50 (40 to 55 min), respectively. The flow rate was 0.4 mL/min, and the injection volume was 25 μL. The UV spectrum was monitored at 280 nm.

Antibody Preparation and Protein Gel Blot Analysis

The 6×His-tagged WLIM1a recombinant proteins purified from BL21 (DE3) strain of *E. coli* were used to immunize rabbits to raise the antibody against WLIM1a. The β-actin and Histone 3 antibody were purchased from Abcam.

Total proteins of soil-grown cotton fibers (1 g) were prepared by extraction with buffer containing 50 mM $NaPO_4$, pH 7.4, 0.5 M NaCl, 1 mM EDTA, 1% (v/v) β-mercaptoethanol, 1 mM PMSF, and 10% polyvinylpolypyrrolidone. About 1 mg of total proteins was obtained. Nuclear proteins were extracted according to the methods described by Marzábal et al. (1998), Zhang et al. (2012), and Deng et al. (2012). Cotton fibers (1 g) from about 100 ovules were ground in liquid nitrogen, and the fine powder was homogenized in 20 mL of buffer A (10 mM HEPES, pH 7.8, 10 mM KCl, 10 mM $MgCl_2$, 5 mM EDTA, 1 mM DTT, 200 μM PMSF, 250 mM Suc, 0.5% Triton X-100, and protease inhibitors). After centrifugation at 4°C for 20 min at 3000*g*, the pellets were washed with buffer A and centrifuged for 15 min at 2000*g*. The pellets were then suspended in 200 μL buffer B (20 mM HEPES, pH 7.8, 20 mM KCl, 1.5 mM $MgCl_2$, 25% glycerol, 200 μM EDTA, 500 μM DTT, 200 μM PMSF, and protease inhibitors), and ~60 μL of buffer C (20 mM HEPES, pH 7.8, 1 M KCl, 1.5 mM $MgCl_2$, 25% glycerol, 200 μM EDTA, 500 μM DTT, 200 μM PMSF, and protease inhibitors) was added to the solution. After centrifugation for 5 min at 12,000*g*, the supernatants were dialyzed against 1000 mL of buffer D (20 mM HEPES, pH 7.8, 100 mM KCl, 10% glycerol, 200 μM EDTA, 500 μM DTT, and 200 μM PMSF) for 1 h. The extract was centrifuged at 12, 000*g* for 30 min. About 100 μg of nuclear proteins was obtained from each sample. Both total and nuclear proteins were quantified by Bradford assay (Bio-Rad protein assay kit), and 40 μg of total or nuclear proteins was subjected to SDS-PAGE. Protein gel blot experiments were performed as reported by J. Wang et al. (2010). The antibodies raised against WLIM1a (1:1000 dilution), mouse β-actin (1:5000 dilution), or mouse Histone 3 (1:5000 dilution) were used as the primary antibodies, and horseradish peroxidase–conjugated goat anti-rabbit/mouse IgG (H+L) (1:3000 dilution; Sungene Biotechnology) was used as a secondary antibody.

Accession Numbers

Sequence data from this article can be found in the GenBank/EMBL data libraries under the following accession numbers: *WLIM1a* (JX648310), *WLIM1b* (ES835442), *WLIM1c* (DW492950), *WLIM2a* (DW506371), *4CL1* (FJ479707), *CCR1* (FJ376603), *CAD6* (NM_119958), Gh-*WLIM5* (JX290321), WLIM1 NM_100894.3 (At1g10200), WLIM2a NM_129548.3 (At2g39900), WLIM2b NM_001035791.1 (At3g55770), PLIM2a NM_001036468.2 (At2g45800), PLIM2b NM_100061.3 (At1g01780), and PLIM2c NM_115987.3 (At3g61230).

Supplemental Data

The following materials are available in the online version of this article.

Supplemental Figure 1. Phenotype Analysis of *WLIM1a*-Transgenic Plants.

Supplemental Figure 2. Comparisons of Cellulose Contents and Expression Levels of Cellulose Synthase Genes between Wild-Type and *WLIM1a*-Transgenic Cotton Fibers.

Supplemental Figure 3. Analysis of the Lignin Contents and Expression Profiles of Phenylpropanoid Biosynthesis Genes in Wild-Type and *WLIM1a*-Underexpressing Cotton Fibers.

Supplemental Figure 4. Deposition of Lignin in the Peduncles of *WLIM1a*-Overexpressing Plants.

Supplemental Figure 5. EMSA Analysis of the DNA Binding Activity of WLIM1a.

Supplemental Figure 6. Measurement of K_d of WLIM1a Protein.

Supplemental Figure 7. Independence of WLIM1a's Actin Bundling Activity on pH and Ca^{2+}.

Supplemental Figure 8. Morphology and F-Actin Organization of Transgenic Tobacco BY2 Cells Overexpressing *WLIM1a*.

Supplemental Figure 9. Quantitative Analysis of the Actin Bundling Extent and Actin Density in BY2 Cells Expressing WLIM1a-GFP and ABD2-mCherry before and after H_2O_2 Treatment.

Supplemental Figure 10. Purity Analysis of Nuclear Proteins Extracted from Cotton Fibers.

Supplemental Table 1. Sequences of the PAL-Box Element in the *4CL1*, *CCR1*, and *CAD6* Promoters.

Supplemental Table 2. Primers Used in This Study.

Supplemental Data Set 1. Text File of the Alignment of Protein Sequences Used for the Phylogenetic Analysis in Figure 1A.

Supplemental Movie 1. Time-Lapse Confocal Scanning Microscopy of a BY2 Cell Coexpressing WLIM1a-GFP and ABD2-mCherry with H_2O_2 Treatment.

Supplemental Movie 2. Time-Lapse Confocal Scanning Microscopy of a BY2 Cell Coexpressing WLIM1a-GFP and ABD2-mCherry without H_2O_2 Treatment.

ACKNOWLEDGMENTS

This work was supported by the Chinese Academy of Sciences (Grant KSCX3-EW-N-03) and the Ministry of Agriculture of China (Grant 2009ZX08005-006B), and by the National Natural Science Foundation

(Grant 31100870). We thank De-Yu Xie (North Carolina State University) for critical reading of the article and Ling Fan (Institute of Nuclear and Biological Technologies, Xinjiang) for helpful discussion on the biosynthesis of lignin-like phenolics in cotton fibers. We also thank Yan-Bao Tian (Institute of Genetics and Developmental Biology, Chinese Academy of Sciences) for technical assistance with confocal microscopy analysis.

AUTHOR CONTRIBUTIONS

G.-X.X., L.-B.H., and H.-Y.W. designed the research. L.-B.H., Y.-B.L., X.-M.W., C.-L.L., and M.L. performed the research. L.-B.H., G.-X.X., H.-Y.W., Y.P., S.-J.W., G.-L.J., and Z.-S.K. analyzed the data. G.-X.X., Z.-S.K., and L.-B.H. wrote the article.

Received August 2, 2013; revised October 11, 2013; accepted October 22, 2013; published November 12, 2013.

REFERENCES

Al-Ghazi, Y., Bourot, S., Arioli, T., Dennis, E.S., and Llewellyn, D.J. (2009). Transcript profiling during fiber development identifies pathways in secondary metabolism and cell wall structure that may contribute to cotton fiber quality. Plant Cell Physiol. **50:** 1364–1381.

Arnaud, D., Déjardin, A., Leplé, J.C., Lesage-Descauses, M.C., and Pilate, G. (2007). Genome-wide analysis of *LIM* gene family in *Populus trichocarpa*, *Arabidopsis thaliana*, and *Oryza sativa*. DNA Res. **14:** 103–116.

Arpat, A.B., Waugh, M., Sullivan, J.P., Gonzales, M., Frisch, D., Main, D., Wood, T., Leslie, A., Wing, R.A., and Wilkins, T.A. (2004). Functional genomics of cell elongation in developing cotton fibers. Plant Mol. Biol. **54:** 911–929.

Baltz, R., Domon, C., Pillay, D.T., and Steinmetz, A. (1992a). Characterization of a pollen-specific cDNA from sunflower encoding a zinc finger protein. Plant J. **2:** 713–721.

Baltz, R., Evrard, J.L., Domon, C., and Steinmetz, A. (1992b). A LIM motif is present in a pollen-specific protein. Plant Cell **4:** 1465–1466.

Beasley, C.A., and Ting, I.P. (1973). The effects of plant growth substances on in vitro fiber development from fertilized cotton ovules. Am. J. Bot. **60:** 130–139.

Boateng, S.Y., Senyo, S.E., Qi, L., Goldspink, P.H., and Russell, B. (2009). Myocyte remodeling in response to hypertrophic stimuli requires nucleocytoplasmic shuttling of muscle LIM protein. J. Mol. Cell. Cardiol. **47:** 426–435.

Boerjan, W., Ralph, J., and Baucher, M. (2003). Lignin biosynthesis. Annu. Rev. Plant Biol. **54:** 519–546.

Brière, C., Bordel, A.C., Barthou, H., Jauneau, A., Steinmetz, A., Alibert, G., and Petitprez, M. (2003). Is the LIM-domain protein HaWLIM1 associated with cortical microtubules in sunflower protoplasts? Plant Cell Physiol. **44:** 1055–1063.

Cave, I.D. (1997). Theory of X-ray measurement of microfibril angle in wood. Wood Sci. Technol. **31:** 143–152.

Dawid, I.B., Toyama, R., and Taira, M. (1995). LIM domain proteins. C. R. Acad. Sci. III **318:** 295–306.

Deng, F.L., Tu, L.L., Tan, J.F., Li, Y., Nie, Y.C., and Zhang, X.L. (2012). GbPDF1 is involved in cotton fiber initiation via the core cis-element HDZIP2ATATHB2. Plant Physiol. **158:** 890–904.

Eliasson, A., Gass, N., Mundel, C., Baltz, R., Kräuter, R., Evrard, J.L., and Steinmetz, A. (2000). Molecular and expression analysis of a LIM protein gene family from flowering plants. Mol. Gen. Genet. **264:** 257–267.

Emons, A.M., and Mulder, B.M. (2000). How the deposition of cellulose microfibrils builds cell wall architecture. Trends Plant Sci. **5:** 35–40.

Fan, L., Shi, W.J., Hu, W.R., Hao, X.Y., Wang, D.M., Yuan, H., and Yan, H.Y. (2009). Molecular and biochemical evidence for phenylpropanoid synthesis and presence of wall-linked phenolics in cotton fibers. J. Integr. Plant Biol. **51:** 626–637.

Gordon, S. (2007). Cotton Fibre Quality. (Boca Raton, FL: CRC Press).

Gou, J.Y., Wang, L.J., Chen, S.P., Hu, W.L., and Chen, X.Y. (2007). Gene expression and metabolite profiles of cotton fiber during cell elongation and secondary cell wall synthesis. Cell Res. **17:** 422–434.

Graves, D.A., and Stewart, J.McD. (1988). Analysis of the protein constituency of developing cotton fibres. J. Exp. Bot. **39:** 59–69.

Hajdukiewicz, P., Svab, Z., and Maliga, P. (1994). The small, versatile pPZP family of Agrobacterium binary vectors for plant transformation. Plant Mol. Biol. **25:** 989–994.

Harholt, J., Jensen, J.K., Sørensen, S.O., Orfila, C., Pauly, M., and Scheller, H.V. (2006). ARABINAN DEFICIENT 1 is a putative arabinosyltransferase involved in biosynthesis of pectic arabinan in Arabidopsis. Plant Physiol. **140:** 49–58.

Hatfield, R., and Fukushima, R.S. (2005). Can lignin be accurately measured? Crop Sci. **45:** 832–839.

He, P., Shan, L., and Sheen, J. (2007). The use of protoplasts to study innate immune responses. Methods Mol. Biol. **354:** 1–9.

Henty, J.L., Bledsoe, S.W., Khurana, P., Meagher, R.B., Day, B., Blanchoin, L., and Staiger, C.J. (2011). *Arabidopsis* actin depolymerizing factor4 modulates the stochastic dynamic behavior of actin filaments in the cortical array of epidermal cells. Plant Cell **23:** 3711–3726.

Higaki, T., Kutsuna, N., Sano, T., Kondo, N., and Hasezawa, S. (2010). Quantification and cluster analysis of actin cytoskeletal structures in plant cells: Role of actin bundling in stomatal movement during diurnal cycles in *Arabidopsis* guard cells. Plant J. **61:** 156–165.

Horsch, R.B., Fry, J.E., Hoffman, N.L., Eichholtz, D., Rogers, S.G., and Fraley, R.T. (1985). A simple and general method for transferring genes into plants. Science **227:** 1229–1231.

Hovav, R., Udall, J.A., Chaudhary, B., Hovav, E., Flagel, L., Hu, G., and Wendel, J.F. (2008). The evolution of spinnable cotton fiber entailed prolonged development and a novel metabolism. PLoS Genet. **4:** e25.

Hussey, P.J., Ketelaar, T., and Deeks, M.J. (2006). Control of the actin cytoskeleton in plant cell growth. Annu. Rev. Plant Biol. **57:** 109–125.

Huwyler, H.R., Franz, G., and Meier, H. (1979). Changes in the composition of cotton fiber cell walls during development. Planta **146:** 635–642.

John, M.E., and Crow, L.J. (1992). Gene expression in cotton (*Gossypium hirsutum* L.) fiber: Cloning of the mRNAs. Proc. Natl. Acad. Sci. USA **89:** 5769–5773.

Kaothien, P., Kawaoka, A., Ebinuma, H., Yoshida, K., and Shinmyo, A. (2002). Ntlim1, a PAL-box binding factor, controls promoter activity of the horseradish wound-inducible peroxidase gene. Plant Mol. Biol. **49:** 591–599.

Kawaoka, A., and Ebinuma, H. (2001). Transcriptional control of lignin biosynthesis by tobacco LIM protein. Phytochemistry **57:** 1149–1157.

Kawaoka, A., Kaothien, P., Yoshida, K., Endo, S., Yamada, K., and Ebinuma, H. (2000). Functional analysis of tobacco LIM protein Ntlim1 involved in lignin biosynthesis. Plant J. **22:** 289–301.

Kim, H.J., and Triplett, B.A. (2001). Cotton fiber growth in planta and in vitro. Models for plant cell elongation and cell wall biogenesis. Plant Physiol. **127:** 1361–1366.

Larkin, M.A., et al. (2007). Clustal W and Clustal X version 2.0. Bioinformatics **23:** 2947–2948.

Li, X.B., Fan, X.P., Wang, X.L., Cai, L., and Yang, W.C. (2005). The cotton *ACTIN1* gene is functionally expressed in fibers and participates in fiber elongation. Plant Cell **17:** 859–875.

Li, X.M., Yuan, D.J., Zhang, J.F., Lin, Z.X., and Zhang, X.L. (2013). Genetic mapping and characteristics of genes specifically or preferentially expressed during fiber development in cotton. PLoS ONE **8:** e54444.

Li, Y., Jiang, J., Li, L., Wang, X.L., Wang, N.N., Li, D.D., and Li, X.B. (2013). A cotton LIM domain-containing protein (GhWLIM5) is involved in bundling actin filaments. Plant Physiol. Biochem. **66:** 34–40.

Liu, C.J. (2012). Deciphering the enigma of lignification: precursor transport, oxidation, and the topochemistry of lignin assembly. Mol. Plant. **5(2):** 304–17.

Luo, M., Xiao, Y.H., Hou, L., Luo, X.Y., Li, D.M., and Pei, Y. (2003). [Cloning and expression analysis of a LIM-domain protein gene from cotton (*Gossypium hirsuturm* L.)]. Yi Chuan Xue Bao **30:** 175–182.

Marzábal, P., Busk, P.K., Ludevid, M.D., and Torrent, M. (1998). The bifactorial endosperm box of gamma-zein gene: Characterisation and function of the Pb3 and GZM cis-acting elements. Plant J. **16:** 41–52.

Meinert, M.C., and Delmer, D.P. (1977). Changes in biochemical composition of the cell wall of the cotton fiber during development. Plant Physiol. **59:** 1088–1097.

Michelot, A., Guérin, C., Huang, S., Ingouff, M., Richard, S., Rodiuc, N., Staiger, C.J., and Blanchoin, L. (2005). The formin homology 1 domain modulates the actin nucleation and bundling activity of *Arabidopsis* FORMIN1. Plant Cell **17:** 2296–2313.

Moes, D., Gatti, S., Hoffmann, C., Dieterle, M., Moreau, F., Neumann, K., Schumacher, M., Diederich, M., Grill, E., Shen, W.H., Steinmetz, A., and Thomas, C. (2013). A LIM domain protein from tobacco involved in actin-bundling and histone gene transcription. Mol. Plant. **6:** 483–502.

Müse, G., Schindler, T., Bergfeld, R., Ruel, K., Acquet, G., Lapierre, C., Speth, V., and Schopfer, P. (1997). Structure and distribution of lignin in primary and secondary cell wallsof maize coleoptiles analyzed by chemical and immunological probes. Planta **201:** 146–159.

Ohta, M., Matsui, K., Hiratsu, K., Shinshi, H., and Ohme-Takagi, M. (2001). Repression domains of class II ERF transcriptional repressors share an essential motif for active repression. Plant Cell **13:** 1959–1968.

Papuga, J., Hoffmann, C., Dieterle, M., Moes, D., Moreau, F., Tholl, S., Steinmetz, A., and Thomas, C. (2010). *Arabidopsis* LIM proteins: A family of actin bundlers with distinct expression patterns and modes of regulation. Plant Cell **22:** 3034–3052.

Potikha, T.S., Collins, C.C., Johnson, D.I., Delmer, D.P., and Levine, A. (1999). The involvement of hydrogen peroxide in the differentiation of secondary walls in cotton fibers. Plant Physiol. **119:** 849–858.

Ruan, Y.L., Llewellyn, D.J., and Furbank, R.T. (2003). Suppression of sucrose synthase gene expression represses cotton fiber cell initiation, elongation, and seed development. Plant Cell **15:** 952–964.

Shi, Y.H., Zhu, S.W., Mao, X.Z., Feng, J.X., Qin, Y.M., Zhang, L., Cheng, J., Wei, L.P., Wang, Z.Y., and Zhu, Y.X. (2006). Transcriptome profiling, molecular biological, and physiological studies reveal a major role for ethylene in cotton fiber cell elongation. Plant Cell **18:** 651–664.

Staiger, C.J., and Blanchoin, L. (2006). Actin dynamics: Old friends with new stories. Curr. Opin. Plant Biol. **9:** 554–562.

Stuart, S., and Evans, R. (1994). X-ray diffraction estimation of the microfibril angle variation in eucalypt wood. Appita. **48:** 197–200.

Tamura, K., Dudley, J., Nei, M., and Kumar, S. (2007). MEGA4: Molecular evolutionary genetics analysis (MEGA) software version 4.0. Mol. Biol. Evol. **24:** 1596–1599.

Thomas, C., Hoffmann, C., Dieterle, M., Van Troys, M., Ampe, C., and Steinmetz, A. (2006). Tobacco WLIM1 is a novel F-actin binding protein involved in actin cytoskeleton remodeling. Plant Cell **18:** 2194–2206.

Traas, J.A., Doonan, J.H., Rawlins, D.J., Shaw, P.J., Watts, J., and Lloyd, C.W. (1987). An actin network is present in the cytoplasm throughout the cell cycle of carrot cells and associates with the dividing nucleus. J. Cell Biol. **105:** 387–395.

Updegraff, D.M. (1969). Semimicro determination of cellulose in biological materials. Anal. Biochem. **32:** 420–424.

Wang, H.J., Wan, A.R., and Jauh, G.Y. (2008). An actin-binding protein, LlLIM1, mediates calcium and hydrogen regulation of actin dynamics in pollen tubes. Plant Physiol. **147:** 1619–1636.

Wang, H.Y., Wang, J., Gao, P., Jiao, G.L., Zhao, P.M., Li, Y., Wang, G.L., and Xia, G.X. (2009). Down-regulation of *GhADF1* gene expression affects cotton fibre properties. Plant Biotechnol. J. **7:** 13–23.

Wang, J., Wang, H.Y., Zhao, P.M., Han, L.B., Jiao, G.L., Zheng, Y.Y., Huang, S.J., and Xia, G.X. (2010). Overexpression of a profilin (GhPFN2) promotes the progression of developmental phases in cotton fibers. Plant Cell Physiol. **51:** 1276–1290.

Wang, Q.Q., Liu, F., Chen, X.S., Ma, X.J., Zeng, H.Q., and Yang, Z.M. (2010). Transcriptome profiling of early developing cotton fiber by deep-sequencing reveals significantly differential expression of genes in a fuzzless/lintless mutant. Genomics **96:** 369–376.

Wang, Z.M., Xue, W., Dong, C.J., Jin, L.G., Bian, S.M., Wang, C., Wu, X.Y., and Liu, J.Y. (2012). A comparative miRNAome analysis reveals seven fiber initiation-related and 36 novel miRNAs in developing cotton ovules. Mol. Plant **5:** 889–900.

Weiskirchen, R., and Günther, K. (2003). The CRP/MLP/TLP family of LIM domain proteins: Acting by connecting. Bioessays **25:** 152–162.

Wu, Y.J., Yan, J., Zhang, R.H., Qu, X.L., Ren, S.L., Chen, N.Z., and Huang, S.J. (2010). *Arabidopsis* FIMBRIN5, an actin bundling factor, is required for pollen germination and pollen tube growth. Plant Cell **22:** 3745–3763.

Xu, B., Gou, J.Y., Li, F.G., Shangguan, X.X., Zhao, B., Yang, C.Q., Wang, L.J., Yuan, S., Liu, C.J., and Chen, X.Y. (2013). A cotton BURP domain protein interacts with α-expansin and their coexpression promotes plant growth and fruit production. Mol. Plant. **6:** 945–958.

Zhang, C., Xu, Y., Guo, S., Zhu, J., Huan, Q., Liu, H., Wang, L., Luo, G., Wang, X., and Chong, K. (2012). Dynamics of brassinosteroid response modulated by negative regulator LIC in rice. PLoS Genet. **8:** e1002686.

Zhang, M., et al. (2011). Spatiotemporal manipulation of auxin biosynthesis in cotton ovule epidermal cells enhances fiber yield and quality. Nat. Biotechnol. **29:** 453–458.

Zhao, P.M., Wang, L.L., Han, L.B., Wang, J., Yao, Y., Wang, H.Y., Du, X.M., Luo, Y.M., and Xia, G.X. (2010). Proteomic identification of differentially expressed proteins in the *Ligon lintless* mutant of upland cotton (*Gossypium hirsutum* L.). J. Proteome Res. **9:** 1076–1087.

Zhao, Q., and Dixon, R.A. (2011). Transcriptional networks for lignin biosynthesis: More complex than we thought? Trends Plant Sci. **16:** 227–233.

Zheng, Q.H., and Zhao, Y. (2007). The diverse biofunctions of LIM domain proteins: Determined by subcellular localization and protein-protein interaction. Biol. Cell **99:** 489–502.

Zhong, R., and Ye, Z.H. (2007). Regulation of cell wall biosynthesis. Curr. Opin. Plant Biol. **10:** 564–572.